

A Flexible Uncertainty Quantification Framework for General Multi-Physics Systems

A. Mittal[†], X. Chen^{*§}, C. H. Tong^{*}, and G. Iaccarino[‡]

Abstract. We present a “module-based hybrid” Uncertainty Quantification (UQ) framework for general non-linear multi-physics simulation. The proposed methodology, introduced in [1], supports the independent development of each *stochastic* linear or nonlinear physics module equipped with the most suitable probabilistic UQ method: non-intrusive, semi-intrusive or intrusive; and provides a generic framework to couple these stochastic simulation components. Moreover, the methodology is illustrated using a common “global” uncertainty representation scheme based on generalized polynomial chaos (gPC) expansions of inputs and outputs. By using thermally-driven cavity flow as the multi-physics model problem, we demonstrate the utility of our framework and report the computational gains achieved.

Key words. Uncertainty Quantification, Polynomial Chaos, Stochastic Modeling, Multi-physics Systems.

AMS subject classifications. 60H15, 60H30, 60H35, 65C30, 65C50

1. Introduction. The discipline of Uncertainty Quantification (UQ) seeks to develop and apply rigorous methodologies to determine uncertainties associated the modeling and simulation of physical processes. The goal is to estimate the probabilistic variations and associated confidence intervals in the quantity of interest resulting from all relevant sources of uncertainty (uncertainty analysis) and to rank the contribution of individual sources of uncertainties (sensitivity analysis). Advances in mathematical/statistical techniques and the availability of high performance computers in recent years have provided an unprecedented opportunity to undertake the computationally intensive task of “model predictions with confidence” in complex multi-physics applications.

Broadly speaking, UQ approaches can be categorized as either non-intrusive or intrusive. Non-intrusive methods such as Monte-Carlo (MC) generate a statistical description of the model output by first drawing random samples from a given probability distribution, running deterministic simulations with those samples, and finally computing the output statistics and/or sensitivities. The main advantages of these methods is the simplicity of implementation using deterministic simulation codes and the embarrassingly parallel computing possibilities. However, these methods suffer from slow convergence rate. Many alternative random sampling designs such as quasi-Monte Carlo [2], Latin Hypercube [3] and importance sampling [4] have been proposed.

Intrusive methods, on the other hand, generally require a re-formulation of deterministic models. A popular class of intrusive methods is the stochastic Galerkin method based on generalized Polynomial Chaos (gPC) expansion [5, 6, 7]. gPC has been used successfully in many applications such as solid mechanics [5], transport in heterogeneous media [8], fluid

*Center for Applied Scientific Computing, Lawrence Livermore National Laboratory, Livermore, CA 94550.

[†]Institute for Computational and Mathematical Engineering, Stanford University, Stanford, CA 94305.

[‡]Mechanical Engineering, Stanford University, Stanford, CA 94305.

[§]Corresponding author (Email: chen73@llnl.gov)

mechanics [9, 10], combustion [11], etc. The advantage of intrusive gPC-based methods is that they may have excellent convergence properties when compared to MC-based methods [12, 13]. However, the rapidly increasing complexity and fidelity of multi-physics models have limited the popularity of intrusive methods. A major reason is that implementation of such methods requires extensive modifications to existing deterministic codes, a task that may be too cumbersome and time-consuming, especially for complex and nonlinearly coupled multi-physics models. The size of the coupled system arising from spatio-temporal discretizations may become so large that the implementation of any further stochastic projection schemes, such as Galerkin (SGS), become computationally intractable. Moreover, additional challenges in implementing intrusive methods yet remain unresolved for complex unsteady applications, such as turbulent flow and highly nonlinear transient problems. For a detailed review of intrusive gPC-based uncertainty propagation for CFD applications, we refer to [9, 14].

To overcome some of these limitations, non-intrusive gPC methods have been proposed as viable alternatives (c.f. [15]). These methods use either regression or quadrature techniques to estimate the coefficients of the gPC expansions and can typically exhibit improved convergence behavior [16] over MC-based methods. In regression-based techniques, oversampling is often required to compute accurate solutions, while in quadrature-based gPC methods, MC-based random sampling is replaced with evaluations corresponding to numerical integration rules (often with very strict constraints). These limitations can render these methods unattractive in practice. Moreover, both intrusive and non-intrusive gPC methods suffer from the so-called curse-of-dimensionality, where the computational effort required grows exponentially with the number of independent sources of uncertainty. Recent developments (stochastic collocation [17, 18], low-rank approximations [19], radial basis functions [20], Pade-Legendre approaches [21], and response surface reconstruction [22]) have demonstrated how the mathematical structure of a model and the regularity of the solutions can be exploited to achieve superlinear convergence [18]. Various “hybrid” approaches that combine intrusive and non-intrusive methods have also been recently proposed. Examples include the multi-state procedure [23], the mixed aleatory/epistemic representation approach [24] and the domain hybridization method [25], the development of which was driven by the need to couple two different descriptions of turbulent flows.

In this article, we propose an alternative hybrid (or partially intrusive) framework for uncertainty propagation in modular multi-physics simulations. Such a framework was initially proposed for linear multi-physics problems in a previous article [1], and we aim to tackle general nonlinear applications in this work. As motivated in [1], the proposed hybrid framework can blend UQ methods, intrusive or non-intrusive that are best suited or available for each individual solver module, and seamlessly “glue” them together to facilitate global uncertainty/sensitivity propagation. To formalize the notion of a modular solution framework, we consider an algebraic system of equations that represents an m -component multi-physics system as follows.

$$(1.1) \quad \mathbf{f}_i(\mathbf{u}_i, \mathbf{u}_1, \dots, \mathbf{u}_{i-1}, \mathbf{u}_{i+1}, \dots, \mathbf{u}_m, \boldsymbol{\xi}_i) = \mathbf{0}, \quad 1 \leq i \leq m,$$

where, $\mathbf{u}_i \in \mathbb{R}^{n_i}$ and $\boldsymbol{\xi}_i \in \mathbb{R}^{s_i}$ correspond to the solution field and input parameters in the i -th component respectively. A differential system of equations can be reduced to the algebraic form in Eq. 1.1 by appropriate discretization schemes in space and time. By implementing

an iterative (staggered) solution approach [26], existing (legacy) solvers for each module i can be leveraged as independent computational kernels to solve Eq. 1.1. At iteration $\ell \geq 0$ and module $1 \leq i \leq m$, we have

$$(1.2) \quad \mathbf{u}_i^{\ell+1}(\boldsymbol{\xi}_1, \dots, \boldsymbol{\xi}_m) = \mathbf{m}_i \left(\mathbf{u}_1^\ell(\boldsymbol{\xi}_1, \dots, \boldsymbol{\xi}_m), \dots, \mathbf{u}_m^\ell(\boldsymbol{\xi}_1, \dots, \boldsymbol{\xi}_m), \boldsymbol{\xi}_i \right).$$

The iterations shown in Eq. 1.2 are performed until each the norm of each solution update $\|\mathbf{u}_i^{\ell+1} - \mathbf{u}_i^\ell\|$ falls below a prescribed tolerance. The solution from the previous iteration step \mathbf{u}_i^ℓ may enter into the i -th module as an initial guess and therefore, has been included as an argument in the module operator \mathbf{m}_i . Therefore, compared to a monolithic approach (fully-coupled solvers) solving Eq. 1.1, the partitioned solution approach only requires the construction of an additional iteration controller which allows individual single-physics modules to be updated and replaced independently. From practical considerations, this approach enables an attractive “plug-and-play” framework for developing multi-physics simulation software. Due to modeling and measurement errors, exact values of the input parameters in Eq. 1.1 are usually not precisely known and therefore, we model these quantities as random variables (with a prescribed statistical description). The goal is to compute uncertainties in the quantities of interest in the form of probability distributions, statistics, and sensitivity information. All these tasks can be efficiently achieved within the proposed hybrid framework using gPC methods.

The remainder of this article is devoted to the description of the proposed module-based hybrid UQ framework. In §2, we provide a brief overview of gPC based intrusive methods, non-intrusive methods, and semi-intrusive methods that exploit additional derivative information. In §3, we detail the module-based hybrid computational framework associated with modular gPC representations. In §4, we demonstrate an implementation our proposed framework thermally driven cavity flows as the numerical multi-physics example.

2. Overview of gPC based UQ methods. Propagating uncertainty and sensitivity information using gPC is a popular choice in cases where the solution is expected to behave regularly in the input stochastic space. We begin this review section by introducing some definitions that will be used throughout the article. Let random inputs $\boldsymbol{\xi}_1, \dots, \boldsymbol{\xi}_m$ belong to a complete probability space $(\Xi, \mathcal{B}(\Xi), \mathcal{P})$, where Ξ is the sample space (set of outcomes), \mathcal{B} denotes the Borel measure and $\mathcal{P} : \Xi \rightarrow [0, 1]$ is a probability measure. We assume that the constituent random scalar components $\xi_{ij} : 1 \leq i \leq m, 1 \leq j \leq s_i$ are independent and belong to a probability space $(\Xi_{ij}, \mathcal{B}(\Xi_{ij}), \mathcal{P}_{ij})$, where $\Xi_{ij} \subseteq \mathbb{R}$. Moreover, we define $\Xi_i = \bigcup_{j=1}^{s_i} \Xi_{ij}$. Furthermore, let $s = \sum_{i=1}^m s_i$ denote the dimension of Ξ . If all the moments of \mathcal{P}_{ij} are finite, then a corresponding set of orthonormal polynomials [27] can be defined as follows.

$$(2.1) \quad \left\{ \psi_{ij}^k : k \geq 0 \right\} : \int_{\mathbb{R}} \psi_{ij}^k(\xi) \psi_{ij}^l(\xi) d\mathcal{P}_{ij}(\xi) = \delta_{kl}.$$

The orthonormality condition gives rise to a three term recurrence property of the polynomials as follows. $\forall \xi \in \Xi_{ij}, k \geq 0$,

$$(2.2) \quad \xi \psi_{ij}^k(\xi) = \sqrt{\beta_{k+1}} \psi_{ij}^{k+1}(\xi) + \alpha_k \psi_{ij}^k(\xi) + \sqrt{\beta_k} \psi_{ij}^{k-1}(\xi)$$

with $\psi_{ij}^{-1} = 0$. The Chebyshev algorithm [27] can be used to obtain the coefficients of the recurrence relation (4) from the raw moments of \mathcal{P}_{ij} . If \mathcal{P}_{ij} is a well known probability measure, the coefficients can be analytically obtained from the Weiner-Askey tables [28]. Once the univariate polynomials are constructed, their multivariate extensions can be naturally constructed by tensorization. We define the component basis polynomials as follows.

$$(2.3) \quad \left\{ \psi_i^{\mathbf{j}} : \mathbf{j} = (j_1 \dots j_{s_i}) \in \mathbb{N}_0^{s_i} \right\} : \psi_i^{\mathbf{j}}(\boldsymbol{\xi}_i) = \psi_i^{\mathbf{j}}(\xi_{i1}, \dots, \xi_{is_i}) = \prod_{k=1}^{s_i} \psi_{ik}^{j_k}(\xi_{ik}).$$

Using the component basis polynomials, we define the global basis polynomials as follows.

$$(2.4) \quad \left\{ \psi^{\mathbf{j}} : \mathbf{j} = (\mathbf{j}_1 \dots \mathbf{j}_m) \in \mathbb{N}_0^{s_1} \times \dots \times \mathbb{N}_0^{s_m} \right\} : \psi^{\mathbf{j}}(\boldsymbol{\xi}_1, \dots, \boldsymbol{\xi}_m) = \prod_{k=1}^m \psi_k^{\mathbf{j}_k}(\boldsymbol{\xi}_k).$$

Assuming that the solution fields in Eq. 1.1 are second order random variables, we can define them in terms of an infinite series of the respective orthonormal polynomials as follows. $\forall 1 \leq i \leq m$,

$$(2.5) \quad \mathbf{u}_i(\boldsymbol{\xi}_1, \dots, \boldsymbol{\xi}_m) = \sum_{|\mathbf{j}| \geq 0} \hat{u}_i^{\mathbf{j}} \psi^{\mathbf{j}}(\boldsymbol{\xi}_1, \dots, \boldsymbol{\xi}_m).$$

Defining a total order $p \geq 0$, we can truncate the infinite series in Eq. 2.5 as follows.

$$(2.6) \quad \mathbf{u}_i^p(\boldsymbol{\xi}_1, \dots, \boldsymbol{\xi}_m) \approx \sum_{|\mathbf{j}|=0}^p \hat{u}_i^{\mathbf{j}} \psi^{\mathbf{j}}(\boldsymbol{\xi}_1, \dots, \boldsymbol{\xi}_m).$$

As stated by the Cameron-Martin theorem [29], if the solution fields are sufficiently regular functions of the random variables, then the truncated approximation \mathbf{u}_i^p converges exponentially to \mathbf{u}_i , in the \mathcal{L}_2 -sense, as $p \rightarrow \infty$. The coefficients of the expansion in equation (6) are known as the global gPC coefficients. The gPC approximations can also be defined using a single-index and matrix-vector product form as follows.

$$(2.7) \quad \mathbf{u}_i^p(\boldsymbol{\xi}_1, \dots, \boldsymbol{\xi}_m) = \sum_{j=0}^P \hat{\mathbf{u}}^j \psi^j(\boldsymbol{\xi}_1, \dots, \boldsymbol{\xi}_m) = \hat{\mathbf{U}}_i \boldsymbol{\psi}(\boldsymbol{\xi}_1, \dots, \boldsymbol{\xi}_m),$$

where $\hat{\mathbf{U}}_i = \hat{\mathbf{U}}_i^p = [\hat{u}_i^0 \dots \hat{u}_i^P]$ denotes the gPC-based coefficient matrix, $\boldsymbol{\psi} = \boldsymbol{\psi}^p = [\psi^0 \dots \psi^P]^{\mathbf{T}}$ denotes the basis vector and $P+1 = \binom{p+s}{p}$ is the cardinality of the basis.

The gPC coefficients have a simple relationship to the first two moments of the solutions, which can be written as follows.

$$(2.8) \quad \begin{aligned} \mathbb{E}(\mathbf{u}_i) &\approx \mathbb{E}(\mathbf{u}_i^p) = \hat{u}_i^0, \\ \text{Cov}(\mathbf{u}_i, \mathbf{u}_i) &\approx \text{Cov}(\mathbf{u}_i^p, \mathbf{u}_i^p) = \sum_{j=1}^P \hat{u}_i^j \left(\hat{u}_i^j \right)^{\mathbf{T}}. \end{aligned}$$

Moreover, since polynomials are orders of magnitude cheaper to compute in comparison to solving the multi-physics system in Eq. 1.1, higher order statistics of the solution fields can be subsequently estimated with exhaustive MC sampling. Similarly, probability distributions of related quantities of interest can be accurately estimated using the kernel density (KDE) method [30]. Furthermore, global sensitivity indices using the ANOVA [31] method can also be directly obtained from the gPC coefficients.

We will now describe how to propagate the gPC coefficients using non-intrusive, semi-intrusive methods and intrusive gPC-based methods. For notational simplicity, the methods will be discussed in the context of a single-physics model, which represents a single component of a multi-physics model, and can be formulated as follows.

$$(2.9) \quad \mathbf{f}(\mathbf{u}, \mathbf{v}, \boldsymbol{\xi}) = \mathbf{0} : \mathbf{f}, \mathbf{u} \in \mathbb{R}^n, \mathbf{v} \in \mathbb{R}^{\tilde{n}}, \boldsymbol{\xi} \in \Xi \subseteq \mathbb{R}^s,$$

where \mathbf{u} is the solution variable, \mathbf{v} is the auxiliary or coupling variable and $\boldsymbol{\xi}$ is the (random) input parameter. The objective here is to compute the solution gPC coefficient matrix $\hat{\mathbf{U}}$ given $\hat{\mathbf{V}} : \mathbf{v} \approx \hat{\mathbf{V}}\boldsymbol{\psi}$.

2.1. Non-intrusive methods. Non-intrusive gPC methods are based on reusing a deterministic solver which can be executed for various input parameter values. For a fixed Q -sized sampling design $\{\boldsymbol{\xi}^{(j)} \in \Xi\}_{j=1}^Q$, we precompute the basis vector samples $\{\boldsymbol{\psi}^{(j)} = \boldsymbol{\psi}(\boldsymbol{\xi}^{(j)})\}_{j=1}^Q$ and construct $\boldsymbol{\Psi} = \boldsymbol{\Psi}^{p,Q} = [\boldsymbol{\psi}^{(1)} \ \dots \ \boldsymbol{\psi}^{(Q)}]$, known as the Fisher matrix [32]. Subsequently, we construct the solution sample matrix $\mathbf{U} = \mathbf{U}^Q = [\mathbf{u}^{(1)} \ \dots \ \mathbf{u}^{(Q)}] : \forall 1 \leq j \leq Q, \mathbf{f}(\mathbf{u}^{(j)}, \hat{\mathbf{V}}\boldsymbol{\psi}^{(j)}, \boldsymbol{\xi}^{(j)}) = \mathbf{0}$. Then, either of the following methods can be used to compute $\hat{\mathbf{U}}$.

2.1.1. Polynomial regression. In this method, $\hat{\mathbf{U}}$ is the analytical solution of a least-squares minimization problem, as follows.

$$(2.10) \quad \hat{\mathbf{U}} = \arg \min_{\hat{\mathbf{Y}} \in \mathbb{R}^{n \times (P+1)}} \left\| \mathbf{U} - \hat{\mathbf{Y}}\boldsymbol{\Psi} \right\|_F = \mathbf{U}\boldsymbol{\Psi}^T (\boldsymbol{\Psi}\boldsymbol{\Psi}^T)^{-1},$$

where $\|\cdot\|_F$ denotes the Frobenius norm. A proof of Eq. 2.10 has been provided in Lemma A1, in Appendix A

To ensure that $\boldsymbol{\Psi}$ is nonsingular, we have the lower bound $Q_{\min} = P + 1$. Moreover, to ensure stability and that the condition number of $\boldsymbol{\Psi}$ remains reasonably low, a sample size of twice the lower bound is typically enforced.

2.1.2. Pseudospectral approximation. Alternatively, we can compute $\hat{\mathbf{U}}$ using numerical integration (quadrature) methods [33]. If $\left\{(\boldsymbol{\xi}^{(j)}, w^{(j)})\right\}_{j=1}^Q$ denotes a quadrature rule in Ξ , we can approximate the gPC coefficient matrix as follows.

$$(2.11) \quad \hat{\mathbf{U}} = \int_{\Xi} \mathbf{u}(\boldsymbol{\xi}) (\boldsymbol{\psi}(\boldsymbol{\xi}))^T d\mathcal{P}(\boldsymbol{\xi}) \approx \sum_{k=1}^Q \mathbf{u}^{(j)} \boldsymbol{\psi}^{(j)}(\boldsymbol{\xi}^{(k)}) w^{(j)} = \mathbf{U}\mathbf{W}\boldsymbol{\Psi}^T,$$

where $\mathbf{W} = \mathbf{W}^Q = \text{diag}\{w^{(1)}, \dots, w^{(Q)}\}$. If the level of the quadrature rule is $\geq p$, the pseudospectral approximation in Eq. 2.11 is equivalent to a weighted regression method using the sample matrix \mathbf{U} . Lemma A2 in Appendix A proves this equivalence.

2.2. Semi-intrusive methods. Semi-intrusive gPC methods are based on extracting additional stochastic information from the model with minimal modifications to the deterministic solver. A popular choice is to extract the first derivatives (gradients) of the solution with respect to the input parameters. In the context of Eq. 2.9, the gradients can be obtained by using the property of the total derivative of \mathbf{f} with respect to the input parameters $\boldsymbol{\xi}$ as follows.

$$(2.12) \quad \frac{\partial \mathbf{f}}{\partial \boldsymbol{\xi}} + \left(\frac{\partial \mathbf{f}}{\partial \mathbf{u}} \right) \frac{\partial \mathbf{u}}{\partial \boldsymbol{\xi}} + \left(\frac{\partial \mathbf{f}}{\partial \mathbf{v}} \right) \frac{\partial \mathbf{v}}{\partial \boldsymbol{\xi}} = \mathbf{0}$$

$$(2.13) \quad \Rightarrow \frac{\partial \mathbf{u}}{\partial \boldsymbol{\xi}} = - \left(\frac{\partial \mathbf{f}}{\partial \mathbf{u}} \right)^{-1} \left(\frac{\partial \mathbf{f}}{\partial \boldsymbol{\xi}} + \left(\frac{\partial \mathbf{f}}{\partial \mathbf{v}} \right) \frac{\partial \mathbf{v}}{\partial \boldsymbol{\xi}} \right).$$

Therefore, the solver would need to be modified slightly to obtain $\frac{\partial \mathbf{f}}{\partial \mathbf{u}}$, $\frac{\partial \mathbf{f}}{\partial \mathbf{v}}$ and $\frac{\partial \mathbf{f}}{\partial \boldsymbol{\xi}}$. If, for instance, Newton's method is used to solve Eq. 2.9, we can simply reuse the Jacobian $\frac{\partial \mathbf{f}}{\partial \mathbf{u}}$ at the last iteration, Moreover, the derivative of \mathbf{v} is approximated as

$$(2.14) \quad \frac{\partial \mathbf{v}}{\partial \boldsymbol{\xi}}(\boldsymbol{\xi}) \approx \hat{\mathbf{V}} \frac{\partial \boldsymbol{\psi}}{\partial \boldsymbol{\xi}}(\boldsymbol{\xi}).$$

Following a similar approach for regression without derivatives, for a fixed Q -sized sampling design $\{\boldsymbol{\xi}^{(j)} \in \Xi\}_{j=1}^Q$, we precompute samples of the basis vectors and their derivatives $\{\tilde{\boldsymbol{\psi}}^{(j)} = \left[\boldsymbol{\psi}^{(j)} \quad \frac{\partial \boldsymbol{\psi}^{(j)}}{\partial \boldsymbol{\xi}} \right]\}_{j=1}^Q$, and construct the modified Fisher matrix that can be written as $\tilde{\boldsymbol{\Psi}} = \tilde{\boldsymbol{\Psi}}^{p,Q} \left[\tilde{\boldsymbol{\psi}}^{(1)} \quad \dots \quad \tilde{\boldsymbol{\psi}}^{(Q)} \right]$. Subsequently, we run the modified solver Q times and construct the solution and derivative sample matrix $\tilde{\mathbf{U}} = \left[\mathbf{u}^{(1)} \quad \frac{\partial \mathbf{u}^{(1)}}{\partial \boldsymbol{\xi}} \quad \dots \quad \mathbf{u}^{(Q)} \quad \frac{\partial \mathbf{u}^{(Q)}}{\partial \boldsymbol{\xi}} \right]$.

To compute the gPC coefficient matrix $\hat{\mathbf{U}}$, we can use the following analytical solution (Lemma A1) of the least-squares minimization problem.

$$(2.15) \quad \hat{\mathbf{U}} = \tilde{\mathbf{U}} \tilde{\boldsymbol{\Psi}}^{\mathbf{T}} \left(\tilde{\boldsymbol{\Psi}} \tilde{\boldsymbol{\Psi}}^{\mathbf{T}} \right)^{-1},$$

To ensure that $\tilde{\boldsymbol{\Psi}}$ is nonsingular, the lower bound on the sample size: $Q_{\min} = \left\lceil \frac{P+1}{s+1} \right\rceil$. For numerical stability, a sample size of twice the lower bound is usually enforced. With the additional first derivative information, the sample size would therefore, be s times smaller than in non-intrusive case without derivative information. Moreover, the additional cost of obtaining the derivatives is an additional s Newton solves, implying that the ratio of computational costs between the semi-intrusive and non-intrusive regression methods would be $\frac{1}{s+1} \left(1 + \frac{s}{k} \right)$, where k is the number of iterations needed to converge to the solution. When $k \gg s$, this ratio is $\approx \frac{1}{s+1}$.

2.3. Intrusive Methods. Intrusive gPC methods are non-sampling methods that propagate the gPC coefficients by solving a single deterministic system of equations which encapsulates all of the uncertainty information. The stochastic Galerkin (SGS) method [6] falls under

the category of intrusive UQ methods and is discussed in the context of a Newton's method used to solve Eq. 2.9. Firstly, we define a gPC approximation of \mathbf{f} as follows.

$$(2.16) \quad \mathbf{f}(\mathbf{u}(\boldsymbol{\xi}), \mathbf{v}(\boldsymbol{\xi}), \boldsymbol{\xi}) \approx \mathbf{f}^P(\boldsymbol{\xi}) = \sum_{j=0}^P \hat{\mathbf{f}}^j \psi^j(\boldsymbol{\xi}) = \hat{\mathbf{F}} \boldsymbol{\psi}(\boldsymbol{\xi}),$$

where

$$(2.17) \quad \hat{\mathbf{F}} = \hat{\mathbf{F}}^P = \begin{bmatrix} \hat{\mathbf{f}}^0 & \dots & \hat{\mathbf{f}}^P \end{bmatrix} = \int_{\Xi} \mathbf{f}(\hat{\mathbf{U}}\boldsymbol{\psi}(\boldsymbol{\xi}), \hat{\mathbf{V}}\boldsymbol{\psi}(\boldsymbol{\xi}), \boldsymbol{\xi}) (\boldsymbol{\psi}(\boldsymbol{\xi}))^T d\mathcal{P}(\boldsymbol{\xi}).$$

Therefore, the deterministic system of equations can be formulated as follows

$$(2.18) \quad \begin{aligned} \hat{\mathbf{f}}^0(\hat{\mathbf{u}}^0, \dots, \hat{\mathbf{u}}^P, \hat{\mathbf{V}}) &= \mathbf{0}, \\ &\vdots \\ \hat{\mathbf{f}}^P(\hat{\mathbf{u}}^0, \dots, \hat{\mathbf{u}}^P, \hat{\mathbf{V}}) &= \mathbf{0}. \end{aligned}$$

A Newton's method, for instance can be used to solve the Eq. 2.18 as follows.

$$(2.19) \quad \begin{bmatrix} \frac{\partial \mathbf{f}^0}{\partial \mathbf{u}^0} & \dots & \frac{\partial \mathbf{f}^0}{\partial \mathbf{u}^P} \\ \vdots & & \vdots \\ \frac{\partial \mathbf{f}^P}{\partial \mathbf{u}^0} & \dots & \frac{\partial \mathbf{f}^P}{\partial \mathbf{u}^P} \end{bmatrix} \begin{bmatrix} \Delta \hat{\mathbf{u}}^0 \\ \vdots \\ \Delta \hat{\mathbf{u}}^P \end{bmatrix} = - \begin{bmatrix} \hat{\mathbf{f}}^0 \\ \vdots \\ \hat{\mathbf{f}}^P \end{bmatrix}.$$

Moreover, we define the gPC approximation of the Jacobian $\mathbf{J} = \frac{\partial \mathbf{f}}{\partial \mathbf{u}}$ in Eq. 2.9 as follows.

$$(2.20) \quad \mathbf{J}(\mathbf{u}(\boldsymbol{\xi}), \mathbf{v}(\boldsymbol{\xi}), \boldsymbol{\xi}) \approx \mathbf{J}^P(\boldsymbol{\xi}) = \sum_{j=0}^P \hat{\mathbf{J}}^j \psi^j(\boldsymbol{\xi}),$$

where $\forall 0 \leq j \leq P$,

$$(2.21) \quad \hat{\mathbf{J}}^j = \int_{\Xi} \mathbf{J}(\hat{\mathbf{U}}\boldsymbol{\psi}(\boldsymbol{\xi}), \hat{\mathbf{V}}\boldsymbol{\psi}(\boldsymbol{\xi}), \boldsymbol{\xi}) \psi^j(\boldsymbol{\xi}) d\mathcal{P}(\boldsymbol{\xi}).$$

Therefore, $\forall 0 \leq j, k \leq P$, the (j, k) -th block (of size $n \times n$) in the Jacobian matrix in Eq. 2.19 can be evaluated as follows.

$$(2.22) \quad \frac{\partial \mathbf{f}^j}{\partial \mathbf{u}^k} = \sum_{l=0}^P \hat{\mathbf{J}}^j c_{jkl} : \forall 0 \leq l \leq P, c_{jkl} = \int_{\Xi} \psi^j(\boldsymbol{\xi}) \psi^k(\boldsymbol{\xi}) \psi^l(\boldsymbol{\xi}) d\mathcal{P}(\boldsymbol{\xi}).$$

Even with the additional overheads of modifying codes from the deterministic solver, solving a single deterministic system in lieu of repeated sampling can be computationally attractive in many instances. However, intrusive methods based on Galerkin projections in the entire global polynomial space are impractical for tackling complex multi-physics systems, where a multidisciplinary developmental strategy is typically employed and ideally, future updates within a particular module should not affect the development of other modules.

3. Module-based hybrid framework for gPC-based UQ. In this section we describe our proposed modular hybrid framework, where we address this particular issue. Within our proposed module-based hybrid framework, individual modules (even those that use intrusive propagation methods) can be developed and managed independently, and incorporated in a plug-and-play fashion (Figure 1).

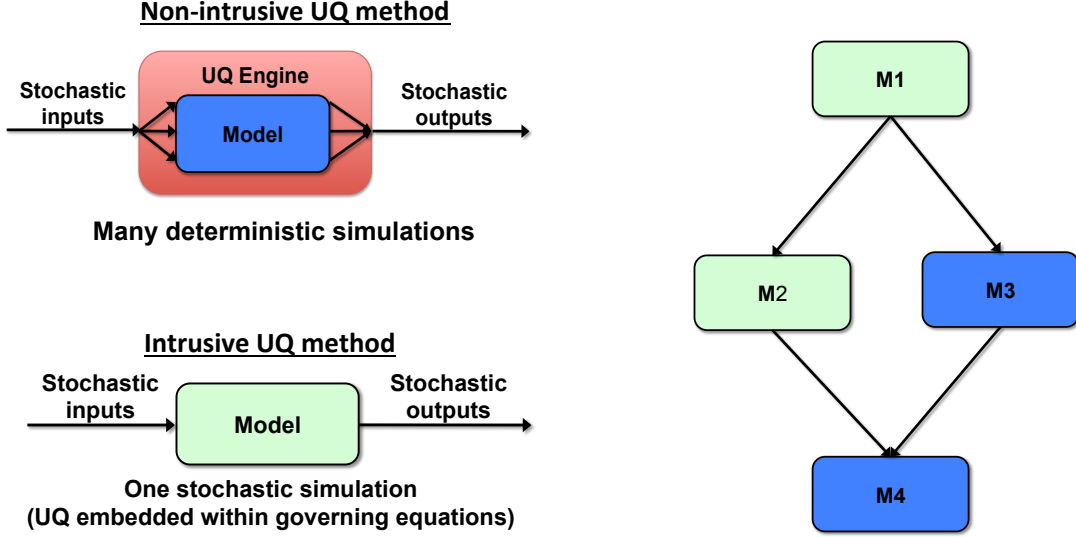


Figure 1. Conceptual illustration of plug-and-play for uncertainty propagation.

Multi-physics models can afford a natural decomposition into subsidiary single-physics models for which modeling expertise and legacy solvers may already exist. From practical considerations, the algorithmic flexibility and modular independence facilitated by this decomposition can significantly reduce developmental costs and overheads for future updates. With the added layer of computational complexity entailed by UQ tasks in predictive simulations, the benefits of modularization become indispensable. Therefore, we propose a framework which facilitates the use of the best suited method of propagating local uncertainty and sensitivity information within each module. To make our discussion concrete, we consider a generic two-module multi-physics model which is bidirectionally coupled i.e. Eq. 1.1 with $M = 2$, and the corresponding staggered solution method employed. Therefore, at each iteration ℓ ,

$$\begin{aligned}
 \mathbf{u}_1^{\ell+1}(\xi_1, \xi_2) &= \mathbf{m}_1(\mathbf{u}_1^\ell(\xi_1, \xi_2), \mathbf{u}_2^\ell(\xi_1, \xi_2), \xi_1) \\
 &= \mathbf{m}_1(\mathbf{y}_1^\ell(\xi_1, \xi_2), \xi_1), \\
 \mathbf{u}_2^{\ell+1}(\xi_1, \xi_2) &= \mathbf{m}_2(\mathbf{u}_1^{\ell+1}(\xi_1, \xi_2), \mathbf{u}_2^\ell(\xi_1, \xi_2), \xi_2) \\
 &= \mathbf{m}_2(\mathbf{y}_2^\ell(\xi_1, \xi_2), \xi_2),
 \end{aligned}
 \tag{3.1}$$

where $\mathbf{y}_1^\ell = [\mathbf{u}_1^\ell; \mathbf{u}_2^\ell]$ and $\mathbf{y}_2^\ell = [\mathbf{u}_1^{\ell+1}; \mathbf{u}_2^\ell]$. Here, we have used the Gauss-Seidel iterative

method, which usually performs better than the standard Jacobi method. The dimensions of the solution fields, operators and stochastic parameters are assumed to be consistent with those defined with respect to the M -module system (1). Since their respective input and output quantities that depend on both ξ_1 and ξ_2 , each module would need to deal with uncertainties that are external to its local parameter space. In general, we can represent the stochastic module operators as follows. $\forall i \in \{1, 2\}$, and iteration ℓ ,

$$(3.2) \quad \hat{U}_i^{\ell+1} = M_i \left(\hat{Y}_i^\ell \right),$$

where $\hat{Y}_1^\ell = [\hat{U}_1^\ell; \hat{U}_2^\ell]$ and $\hat{Y}_2^\ell = [\hat{U}_1^{\ell+1}; \hat{U}_2^\ell]$.

In a monolithic intrusive propagation framework, any changes made in characterizing the probability spaces of ξ_1 or ξ_2 would need to be reflected in both M_1 and M_2 . In our proposed framework, our algorithmic goal is to make each module “self-inclusive” in its implementation and flexible in its methodology for propagating the local stochastic information. Thereby, we would retain module independence and any changes made to the set of local uncertainties in a module would not affect the development of other modules. Towards this end, we need to derive the necessary operators which transform between global and modular representations of stochastic information. In general, we can represent these transformations as follows.

$$(3.3) \quad \hat{U}_i^{\ell+1} = \sum_{j=1}^{N_1} \Phi_{ij}^{-1} \circ \tilde{M}_{ij} \left(\Phi_{ij} \circ \hat{Y}_i^\ell \right),$$

where Φ_{ij} denotes the *restriction* map in module i to subproblem j and Φ_{ij}^{-1} denotes the reverse *prolongation* map. Moreover, \tilde{M}_{ij} represents the stochastic module operator based on \mathbf{m}_i which depends on ξ_i or Ξ_i , depending on the type of uncertainty propagation method employed.

For linear multi-physics models, a decomposition property of linear modules can be exploited such that the computation of the gPC coefficients at the next iteration can be split into independent subproblems of smaller size (corresponding to different external indices for the external polynomial basis functions). Besides the truncation error imposed by the gPC approximation, this decomposition does not suffer from any additional loss of stochastic information. A proof of this property has been provided in the previous work [1], but limited to the case when the input parameters in each module are scalars. Lemma A3 and Lemma A4 in Appendix A prove the general case when the input parameters are vectors, in the context of non-intrusive and intrusive projection methods respectively.

We now consider a general nonlinear model setup for intrusive spectral projection, for which the corresponding restriction and prolongation maps will be defined. In each module, the local stochastic information can be represented using a *modular* gPC approximation of the input/output data.

3.1. Modular gPC approximation. For a given order p , let $\psi \equiv \psi^p$ denote as the global polynomial basis vector with $\psi_1 \equiv \psi_1^p$ and $\psi_2 \equiv \psi_2^p$ denoting the modular polynomial basis vectors. Therefore, we can relate the global and modular gPC approximations as follows.

$\forall i \in \{1, 2\}$,

$$\begin{aligned}
\mathbf{u}_i^p(\boldsymbol{\xi}_1, \boldsymbol{\xi}_2) &= \sum_{|\mathbf{j}|=0}^p \hat{\mathbf{u}}_i^{\mathbf{j}_1 \mathbf{j}_2} \psi_1^{\mathbf{j}_1}(\boldsymbol{\xi}_1) \psi_2^{\mathbf{j}_2}(\boldsymbol{\xi}_2) = \hat{\mathbf{U}}_i \boldsymbol{\psi}(\boldsymbol{\xi}_1, \boldsymbol{\xi}_2) \\
&= \sum_{|\mathbf{j}|=0}^p \tilde{\mathbf{u}}_{i,1}^{\mathbf{j}}(\boldsymbol{\xi}_2) \psi_1^{\mathbf{j}}(\boldsymbol{\xi}_1) = \tilde{\mathbf{U}}_{i,1}(\boldsymbol{\xi}_2) \boldsymbol{\psi}_1(\boldsymbol{\xi}_1) \\
(3.4) \quad &= \sum_{|\mathbf{j}|=0}^p \tilde{\mathbf{u}}_{i,2}^{\mathbf{j}}(\boldsymbol{\xi}_1) \psi_2^{\mathbf{j}}(\boldsymbol{\xi}_2) = \tilde{\mathbf{U}}_{i,2}(\boldsymbol{\xi}_1) \boldsymbol{\psi}_2(\boldsymbol{\xi}_2),
\end{aligned}$$

where $\tilde{\mathbf{U}}_{i,1}$ and $\tilde{\mathbf{U}}_{i,2}$ are the modular gPC coefficient matrices in module 1 and module 2 respectively. Subsequently, the restriction and prolongation maps are defined to transform between global and modular gPC matrices.

Since implementation of the intrusive stochastic modules is only based on the local stochastic information contained in the inputs and output data, the restriction map transforms the global gPC coefficient matrix to the module gPC coefficient matrix at various sampling points in the external stochastic parameter space. Let $P+1 = \binom{s+p}{p}$ denote the total number of global basis polynomials and $P_i+1 = \binom{s_i+p}{p} : i \in \{1, 2\}$ denote the total number of modular basis polynomials in module i .

Considering module 1, for instance, we define the set of samples $\{\boldsymbol{\xi}_2^{(j)}\}_{j=1}^{Q_2}$. Subsequently, we can define the restriction map as follows. $\forall i \in \{1, 2\}, 1 \leq j \leq Q_2$,

$$(3.5) \quad \tilde{\mathbf{U}}_{i,1}(\boldsymbol{\xi}_2^{(j)}) = \Phi_{1j} \circ \hat{\mathbf{U}}_i = \hat{\mathbf{U}}_i \mathbf{P}_1 \boldsymbol{\Pi}_1(\boldsymbol{\xi}_2^{(j)}),$$

where $\boldsymbol{\Pi}_1 : \forall \boldsymbol{\xi}_2 \in \Xi_2$,

$$(3.6) \quad \boldsymbol{\Pi}_1(\boldsymbol{\xi}_2) = \begin{bmatrix} \psi_2^{p-|\mathbf{j}_0|}(\boldsymbol{\xi}_2) & & \\ & \ddots & \\ & & \psi_2^{p-|\mathbf{j}_{P_1}|}(\boldsymbol{\xi}_2) \end{bmatrix}$$

is a $(P+1) \times (P_1+1)$ sparse transformation matrix with at most P non-zero entries. Moreover, \mathbf{P}_1 is the corresponding permutation matrix and $\forall 0 \leq k \leq P_1, \mathbf{j}_k \in \mathbb{N}_0^{s_1} : 0 \leq |\mathbf{j}_k| \leq p$ and $|\mathbf{j}_0| \leq \dots \leq |\mathbf{j}_{P_1}|$.

For any $\mathbf{u} : \Xi \rightarrow \mathbb{R}^n$, the corresponding global gPC coefficient matrix can be approximated as follows.

$$(3.7) \quad \hat{\mathbf{U}} \approx \sum_{i=1}^{Q_2} \Phi_{1j}^{-1} \circ \tilde{\mathbf{U}}_1(\boldsymbol{\xi}_2^{(j)}) \quad \text{or} \quad \hat{\mathbf{U}} \approx \sum_{i=1}^{Q_1} \Phi_{2j}^{-1} \circ \tilde{\mathbf{U}}_2(\boldsymbol{\xi}_1^{(j)})$$

where the prolongation map Φ_{ij}^{-1} can be defined using either a least-squares regression the pseudospectral approach, as provided Theorem 1 and Theorem 2 respectively.

Theorem 1.: Given a sufficiently large number of samples of the modular gPC coefficient matrices $\left\{ \tilde{\mathbf{U}}_1 \left(\boldsymbol{\xi}_2^{(j)} \right) \right\}_{j=1}^{Q_2}$ of a function $\mathbf{u} : \Xi \rightarrow \mathbb{R}^n$, a least-square recovery of the global gPC coefficient matrix can be obtained, according to Eq. 3.7, using the prolongation map $\Phi_{1j}^{-1} : \forall 1 \leq j \leq Q_2$,

$$(3.8) \quad \Phi_{1j}^{-1} \circ \tilde{\mathbf{U}}_1 \left(\boldsymbol{\xi}_2^{(j)} \right) = \tilde{\mathbf{U}}_1 \left(\boldsymbol{\xi}_2^{(j)} \right) \boldsymbol{\Pi}_1 \left(\boldsymbol{\xi}_2^{(j)} \right)^{\mathbf{T}} \mathbf{V}_1^{-1} \mathbf{P}_1^{\mathbf{T}},$$

where

$$(3.9) \quad \mathbf{V}_1 = \sum_{j=1}^{Q_2} \boldsymbol{\Pi}_1 \left(\boldsymbol{\xi}_2^{(j)} \right) \boldsymbol{\Pi}_1 \left(\boldsymbol{\xi}_2^{(j)} \right)^{\mathbf{T}}.$$

Proof.: A least-squares recovery on the global gPC coefficient matrix can be formulated as the following minimization problem.

$$(3.10) \quad \hat{\mathbf{U}} = \arg \min_{\hat{\mathbf{Y}} \in \mathbb{R}^{n \times (P+1)}} \left\| \begin{bmatrix} \tilde{\mathbf{U}}_1 \left(\boldsymbol{\xi}_2^{(1)} \right) - \hat{\mathbf{Y}} \mathbf{P}_1 \boldsymbol{\Pi}_1 \left(\boldsymbol{\xi}_2^{(1)} \right) \\ \vdots \\ \tilde{\mathbf{U}}_1 \left(\boldsymbol{\xi}_2^{(Q)} \right) - \hat{\mathbf{Y}} \mathbf{P}_1 \boldsymbol{\Pi}_1 \left(\boldsymbol{\xi}_2^{(Q)} \right) \end{bmatrix} \right\|_F.$$

The derivation in Lemma A1 can be used to prove Eq.3.8 as follows.

$$(3.11) \quad \begin{aligned} \hat{\mathbf{U}} &= \begin{bmatrix} \tilde{\mathbf{U}}_1 \left(\boldsymbol{\xi}_2^{(1)} \right) & \cdots & \tilde{\mathbf{U}}_1 \left(\boldsymbol{\xi}_2^{(Q)} \right) \end{bmatrix} \begin{bmatrix} \boldsymbol{\Pi}_1 \left(\boldsymbol{\xi}_2^{(1)} \right) \\ \vdots \\ \boldsymbol{\Pi}_1 \left(\boldsymbol{\xi}_2^{(Q)} \right) \end{bmatrix}^{\mathbf{T}} \\ &\times \left(\begin{bmatrix} \boldsymbol{\Pi}_1 \left(\boldsymbol{\xi}_2^{(1)} \right) & \cdots & \boldsymbol{\Pi}_1 \left(\boldsymbol{\xi}_2^{(Q)} \right) \end{bmatrix} \begin{bmatrix} \boldsymbol{\Pi}_1 \left(\boldsymbol{\xi}_2^{(1)} \right) \\ \vdots \\ \boldsymbol{\Pi}_1 \left(\boldsymbol{\xi}_2^{(Q)} \right) \end{bmatrix}^{\mathbf{T}} \right)^{-1} \mathbf{P}_1^{\mathbf{T}} \\ &= \begin{bmatrix} \tilde{\mathbf{U}}_1 \left(\boldsymbol{\xi}_2^{(1)} \right) & \cdots & \tilde{\mathbf{U}}_1 \left(\boldsymbol{\xi}_2^{(Q)} \right) \end{bmatrix} \begin{bmatrix} \boldsymbol{\Pi}_1 \left(\boldsymbol{\xi}_2^{(1)} \right) \\ \vdots \\ \boldsymbol{\Pi}_1 \left(\boldsymbol{\xi}_2^{(Q)} \right) \end{bmatrix}^{\mathbf{T}} \mathbf{V}_1^{-1} \mathbf{P}_1^{\mathbf{T}} \\ &= \sum_{j=1}^{Q_2} \tilde{\mathbf{U}}_1 \left(\boldsymbol{\xi}_2^{(j)} \right) \boldsymbol{\Pi}_1 \left(\boldsymbol{\xi}_2^{(j)} \right)^{\mathbf{T}} \mathbf{V}_1^{-1} \mathbf{P}_1^{\mathbf{T}}. \end{aligned}$$

Therefore, combining Eq. 3.7 and Eq. 3.11 yields Eq. 3.8. \square

Theorem 2.: Given a quadrature rule $\left\{ \left(\boldsymbol{\xi}_2^{(j)}, w_2^{(j)} \right) \right\}_{j=1}^{Q_2}$, which can exactly integrate polynomials with total degree $\leq 2p$, and the corresponding samples of the modular gPC coefficient matrices $\left\{ \tilde{\mathbf{U}}_1 \left(\boldsymbol{\xi}_2^{(j)} \right) \right\}_{j=1}^{Q_2}$ of a function $\mathbf{u} : \Xi \rightarrow \mathbb{R}^n$, a pseudospectral recovery of the global gPC coefficient matrix can be obtained, according to Eq. 3.7, using the prolongation map $\Phi_{1j}^{-1} : \forall 1 \leq j \leq Q_2$,

$$(3.12) \quad \Phi_{1j}^{-1} \circ \tilde{\mathbf{U}}_1 \left(\boldsymbol{\xi}_2^{(j)} \right) = w_2^{(j)} \tilde{\mathbf{U}}_1 \left(\boldsymbol{\xi}_2^{(j)} \right) \mathbf{\Pi}_1 \left(\boldsymbol{\xi}_2^{(j)} \right)^{\mathbf{T}} \mathbf{P}_1^{\mathbf{T}}.$$

Proof.: Since $\mathbf{\Pi}_1$ contains polynomials of total degree less than or equal to p , we have

$$(3.13) \quad \int_{\mathbb{R}^{s_2}} \mathbf{\Pi}_1 \left(\boldsymbol{\xi}_2 \right) \mathbf{\Pi}_1 \left(\boldsymbol{\xi}_2 \right)^{\mathbf{T}} d\mathcal{P} \left(\boldsymbol{\xi}_2 \right) = \sum_{j=1}^{Q_2} w_2^{(j)} \mathbf{\Pi}_1 \left(\boldsymbol{\xi}_2^{(j)} \right) \mathbf{\Pi}_1 \left(\boldsymbol{\xi}_2^{(j)} \right)^{\mathbf{T}} = \mathbf{I}_{P+1}.$$

Therefore, we have

$$(3.14) \quad \begin{aligned} \hat{\mathbf{U}} &= \hat{\mathbf{U}} \mathbf{P}_1 \left(\int_{\mathbb{R}^{s_2}} \mathbf{\Pi}_1 \left(\boldsymbol{\xi}_2 \right) \mathbf{\Pi}_1 \left(\boldsymbol{\xi}_2 \right)^{\mathbf{T}} d\mathcal{P} \left(\boldsymbol{\xi}_2 \right) \right) \mathbf{P}_1^{\mathbf{T}} \\ &= \left(\int_{\mathbb{R}^{s_2}} \hat{\mathbf{U}} \mathbf{P}_1 \mathbf{\Pi}_1 \left(\boldsymbol{\xi}_2 \right) \mathbf{\Pi}_1 \left(\boldsymbol{\xi}_2 \right)^{\mathbf{T}} d\mathcal{P} \left(\boldsymbol{\xi}_2 \right) \right) \mathbf{P}_1^{\mathbf{T}} \\ &= \left(\int_{\mathbb{R}^{s_2}} \tilde{\mathbf{U}}_1 \left(\boldsymbol{\xi}_2 \right) \mathbf{\Pi}_1 \left(\boldsymbol{\xi}_2 \right)^{\mathbf{T}} d\mathcal{P} \left(\boldsymbol{\xi}_2 \right) \right) \mathbf{P}_1^{\mathbf{T}} \\ &= \sum_{j=1}^{Q_2} w_2^{(j)} \tilde{\mathbf{U}}_1 \left(\boldsymbol{\xi}_2^{(j)} \right) \mathbf{\Pi}_1 \left(\boldsymbol{\xi}_2^{(j)} \right)^{\mathbf{T}} \mathbf{P}_1^{\mathbf{T}}. \end{aligned}$$

Therefore, combining Eq. 3.7 and Eq. 3.14 yields Eq. 3.12. \square

Similarly, we can define the restriction and prolongation maps corresponding to module 2. These maps provide the basic components of our proposed module-based hybrid framework and their specific definition depends on the problem structure and uncertainty propagation method employed in each module. In the context of Eq. 3.3. we will now summarize these definitions for the uncertainty propagation methods discussed in section 2.

3.2. Restriction and prolongation map definitions. For linear problems, we have $N_1 = P_2 + 1$, $N_2 = P_1 + 1$. $\forall i \in \{1, 2\}$, let $\mathcal{J}_i \equiv \left\{ \mathbf{j}_j \in \mathbb{N}_0^{s_i} : 0 \leq |\mathbf{j}_j| \leq p \right\}_{j=1}^{P_i+1}$ denote the internal index set, $\mathcal{K}_i \equiv \left\{ \mathbf{k}_j \in \mathbb{N}_0^{s-i} : 0 \leq |\mathbf{k}_j| \leq p \right\}_{j=1}^{N_i}$ denote the external index set and $\mathcal{I}_i \equiv \left\{ \mathbf{j}_j \mathbf{k}_j \right\}_{j=1}^{P+1}$ denote the global index set. Subsequently, $\forall i \in \{1, 2\}, 1 \leq j \leq N_i$, and iteration ℓ , we have

$$(3.15) \quad \begin{aligned} \Phi_{ij} \circ \hat{\mathbf{Y}}_i^\ell &= \hat{\mathbf{Y}}_i^\ell \mathbf{P}_i \mathbf{E}_j, \\ \Phi_{ij}^{-1} \circ \tilde{\mathbf{M}}_{ij} &= \tilde{\mathbf{M}}_{ij} \mathbf{E}_j^{\mathbf{T}} \mathbf{P}_i^{\mathbf{T}}, \end{aligned}$$

where the columns in \mathbf{E}_j are a subset of the columns (unit vectors) in \mathbf{I}_{P+1} such that

$$(3.16) \quad \mathbf{E}_j = \left[\cdots \quad \mathbf{e}_k \quad \cdots \right] : \mathbf{j}_k \mathbf{k}_j \in \mathcal{I}_i.$$

Moreover, we define $\hat{Y}_{i,j}^\ell = \Phi_{ij} \circ \hat{Y}_i^\ell$, $\psi_{i,j} = \psi_i^{p-|k_j|}$, $\Psi_{i,j} = \Psi_i^{p-|k_j|}$, $\tilde{\psi}_{i,j} = \tilde{\psi}_i^{p-|k_j|}$, $\tilde{\Psi}_{i,j} = \tilde{\Psi}_i^{p-|k_j|}$ and \tilde{m}_i as the modified i -th module with its outputs $\left[\mathbf{u}_i^{\ell+1} \quad \frac{\partial \mathbf{u}_i^{\ell+1}}{\partial \boldsymbol{\xi}_i} \right]$. Subsequently, we can define \tilde{M}_{ij} , based on the uncertainty propagation method used in module i , as follows.

I. Non-intrusive regression: We have

$$(3.17) \quad \tilde{M}_{ij}(\hat{Y}_{i,j}^\ell) = \left(\sum_{l=1}^{Q_{i,j}} \mathbf{m}_i(\hat{Y}_{i,j}^\ell \psi_{i,j}(\boldsymbol{\xi}_i^{(l)})) \psi_{i,j}(\boldsymbol{\xi}_i^{(l)})^\mathbf{T} \right) (\Psi_{i,j} \Psi_{i,j}^\mathbf{T})^{-1}$$

II. Non-intrusive projection: We have

$$(3.18) \quad \tilde{M}_{ij}(\hat{Y}_{i,j}^\ell) = \sum_{l=1}^{Q_{i,j}} w_i^{(l)} \mathbf{m}_i(\hat{Y}_{i,j}^\ell \psi_{i,j}(\boldsymbol{\xi}_i^{(l)})) \psi_{i,j}(\boldsymbol{\xi}_i^{(l)})^\mathbf{T}.$$

III. Semi-intrusive regression: We have

$$(3.19) \quad \tilde{M}_{ij}(\hat{Y}_{i,j}^\ell) = \left(\sum_{l=1}^{Q_{i,j}} \tilde{m}_i(\hat{Y}_{i,j}^\ell \tilde{\psi}_{i,j}(\boldsymbol{\xi}_i^{(l)})) \tilde{\psi}_{i,j}(\boldsymbol{\xi}_i^{(l)})^\mathbf{T} \right) (\tilde{\Psi}_{i,j} \tilde{\Psi}_{i,j}^\mathbf{T})^{-1}.$$

IV. Intrusive projection: From Lemma A4, we have

$$(3.20) \quad \begin{aligned} & \left(\int_{\Xi_i} (\psi_{i,j}(\boldsymbol{\xi}_i) \psi_{i,j}(\boldsymbol{\xi}_i)^\mathbf{T}) \otimes \mathbf{A}_i(\boldsymbol{\xi}_i) d\mathcal{P}_i(\boldsymbol{\xi}_i) \right) \text{vec}(\tilde{M}_{ij}(\hat{Y}_{i,j}^\ell)) \\ &= \int_{\Xi_i} \psi_{i,j}(\boldsymbol{\xi}_i) \otimes \mathbf{b}_i(\hat{Y}_{i,j}^\ell \psi_{i,j}^j(\boldsymbol{\xi}_i), \boldsymbol{\xi}_i) d\mathcal{P}_i(\boldsymbol{\xi}_i). \end{aligned}$$

As opposed to linear problems, the definition of restriction and prolongation maps in nonlinear problems would depend on the uncertainty propagation method used in the respective modules.

I. Non-intrusive regression: We define $N_i = Q$ and

$$(3.21) \quad \begin{aligned} \Phi_{ij} \circ \hat{Y}_i^\ell &= \hat{Y}_i^\ell \mathbf{P}_i \psi(\boldsymbol{\xi}^{(j)}), \\ \tilde{M}_{ij}(\Phi_{ij} \circ \hat{Y}_i^\ell) &= \mathbf{m}_i(\Phi_{ij} \circ \hat{Y}_i^\ell, \boldsymbol{\xi}_i^{(j)}), \\ \Phi_{ij}^{-1} \circ \tilde{M}_{ij} &= \tilde{M}_{ij} \psi(\boldsymbol{\xi}^{(j)})^\mathbf{T} (\Psi \Psi^\mathbf{T})^{-1} \mathbf{P}_i^\mathbf{T}. \end{aligned}$$

II. Non-intrusive projection: We define $N_i = Q$ and

$$(3.22) \quad \begin{aligned} \Phi_{ij} \circ \hat{Y}_i^\ell &= \hat{Y}_i^\ell \mathbf{P}_i \psi(\boldsymbol{\xi}^{(j)}), \\ \tilde{M}_{ij}(\Phi_{ij} \circ \hat{Y}_i^\ell) &= \mathbf{m}_i(\Phi_{ij} \circ \hat{Y}_i^\ell, \boldsymbol{\xi}_i^{(j)}), \\ \Phi_{ij}^{-1} \circ \tilde{M}_{ij} &= w^{(j)} \tilde{M}_{ij} \psi(\boldsymbol{\xi}^{(j)})^\mathbf{T} \mathbf{P}_i^\mathbf{T}. \end{aligned}$$

III. Semi-intrusive regression: We define $N_i = Q_i$ and

$$(3.23) \quad \begin{aligned} \Phi_{ij} \circ \hat{Y}_i^\ell &= \hat{Y}_i^\ell P_i \tilde{\psi}_i(\boldsymbol{\xi}^{(j)}), \\ \tilde{M}_{ij}(\Phi_{ij} \circ \hat{Y}_i^\ell) &= \tilde{m}_i(\Phi_{ij} \circ \hat{Y}_i^\ell, \boldsymbol{\xi}_i^{(j)}), \\ \Phi_{ij}^{-1} \circ \tilde{M}_{ij} &= \tilde{M}_{ij} \tilde{\psi}_i(\boldsymbol{\xi}^{(j)})^\mathbf{T} (\tilde{\Psi}_i \tilde{\Psi}_i^\mathbf{T})^{-1} P_i^\mathbf{T}. \end{aligned}$$

IV. Intrusive projection: We define $N_1 = Q_2$ and $N_2 = Q_1$, the restriction map Φ_{ij} using Eq. 3.5, the prolongation map Φ_{ij}^{-1} using either Eq. 3.8 or Eq. 3.12, and \tilde{M}_{ij} :

$$(3.24) \quad \begin{aligned} &\left(\int_{\Xi_i} (\boldsymbol{\psi}_i(\boldsymbol{\xi}_i) \boldsymbol{\psi}_i(\boldsymbol{\xi}_i)^\mathbf{T}) \otimes \frac{\partial \mathbf{f}_i}{\partial \mathbf{u}_i}(\Phi_{ij} \circ \hat{Y}_i^\ell \boldsymbol{\psi}_i(\boldsymbol{\xi}_i), \boldsymbol{\xi}_i) d\mathcal{P}_i(\boldsymbol{\xi}_i) \right) \\ &\times \text{vec} \left(\tilde{M}_{ij}(\Phi_{ij} \circ \hat{Y}_i^\ell) - \Phi_{ij} \circ \hat{U}_i^\ell \right) \\ &= - \int_{\Xi_i} \boldsymbol{\psi}_i(\boldsymbol{\xi}_i) \otimes \mathbf{f}_i(\Phi_{ij} \circ \hat{Y}_i^\ell \boldsymbol{\psi}_i(\boldsymbol{\xi}_i), \boldsymbol{\xi}_i) d\mathcal{P}_i(\boldsymbol{\xi}_i). \end{aligned}$$

4. Numerical example. In this section, we demonstrate an implementation of our proposed framework using a thermally driven cavity flow problem as a multi-physics simulation problem, with uncertain boundary conditions and fluid properties.

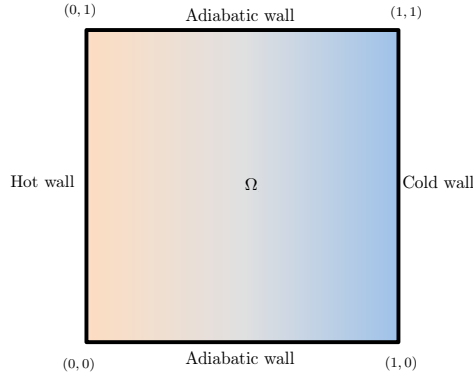


Figure 2. Computational domain for the thermally-driven cavity flow problem.

4.1. Model setup. Firstly, we consider a 2D square cavity $\Omega = (0, 1)_{r_1} \times (0, 1)_{r_2}$ in which the non-dimensional fluid velocity $\mathbf{u} = [u_1 \ u_2]^\mathbf{T}$, pressure p , and temperature T are governed by the incompressible Boussinesq equations [34]:

$$(4.1) \quad \begin{aligned} \nabla^\mathbf{T} \mathbf{u}(\mathbf{x}, \boldsymbol{\xi}) &= 0, \\ \left(\mathbf{u}(\mathbf{x}, \boldsymbol{\xi})^\mathbf{T} \nabla \right) \mathbf{u}(\mathbf{x}, \boldsymbol{\xi}) + \nabla p(\mathbf{x}, \boldsymbol{\xi}) \\ - \text{Pr} \nabla^\mathbf{T} \nabla \mathbf{u}(\mathbf{x}, \boldsymbol{\xi}) - \text{PrRa}(\mathbf{x}, \boldsymbol{\xi}_1) T(\mathbf{x}, \boldsymbol{\xi}) \mathbf{e}_2 &= \mathbf{0}, \\ \left(\mathbf{u}(\mathbf{x}, \boldsymbol{\xi})^\mathbf{T} \nabla \right) T(\mathbf{x}, \boldsymbol{\xi}) - \nabla^\mathbf{T} \nabla T(\mathbf{x}, \boldsymbol{\xi}) &= 0, \quad \mathbf{x} \in \Omega, \end{aligned}$$

with homogenous Dirichlet boundary conditions for \mathbf{u} and Neumann boundary conditions for p at all boundaries. Moreover, the boundary conditions for temperature (Figure 2) are prescribed as follows.

$$(4.2) \quad \begin{aligned} \frac{\partial T}{\partial x_2}(x_1, 0, \boldsymbol{\xi}) &= \frac{\partial T}{\partial x_2}(x_1, 1, \boldsymbol{\xi}) = 0, & x_1 &\in [0, 1], \\ T(0, x_2, \boldsymbol{\xi}) - T_h(x_2, \boldsymbol{\xi}_2) &= T(1, x_2, \boldsymbol{\xi}) = 0, & x_2 &\in [0, 1]. \end{aligned}$$

Moreover, \mathbf{e}_2 denotes $[0 \ 1]^T$ while Pr and Ra denote the Prandtl and Rayleigh numbers respectively, T_h denotes the hot-wall temperature such that $\forall x_2 \in [0, 1]$,

$$(4.3) \quad T_h(x_2, \boldsymbol{\xi}_2) = \bar{T}_h + h(x_2, \boldsymbol{\xi}_2) \sin^2(\pi x_2),$$

where \bar{T}_h is the mean hot-wall temperature and h denotes the perturbation amplitude.

In this study, Ra and h are assumed to be independent random fields, and modeled using the following Karhunen-Loeve (KL) [35] expansions. $\forall \mathbf{x} \in \Omega, \boldsymbol{\xi}_1 \in \Xi_1$,

$$(4.4) \quad \text{Ra}(\mathbf{x}, \boldsymbol{\xi}_1) = \bar{\text{Ra}} + \sqrt{3}\delta_{\text{Ra}} \sum_{j=1}^{s_1} \gamma_{\text{Ra},j}(\mathbf{x}) \xi_{1j},$$

where $\bar{\text{Ra}}$ denotes the mean of Ra and $\{\xi_{1j} \sim U[-1, 1]\}_{j=1}^{s_1}$ are *i.i.d* random variables. Similarly, $\forall x_2 \in (0, 1), \boldsymbol{\xi}_2 \in \Xi_2$,

$$(4.5) \quad h(x_2, \boldsymbol{\xi}_2) = \sqrt{3}\delta_h \sum_{j=1}^{s_2} \gamma_{h,j}(x_2) \xi_{2j},$$

where $\{\xi_{2j} \sim U[-1, 1]\}_{j=1}^{s_2}$ are *i.i.d* random variables. Moreover, we assume that both Ra and h have exponential kernels

$$(4.6) \quad \begin{aligned} C_{\text{Ra}}(\mathbf{x}, \mathbf{y}) &= \delta_{\text{Ra}}^2 \exp\left(-\frac{\|\mathbf{x} - \mathbf{y}\|_1}{l_{\text{Ra}}}\right), \mathbf{x}, \mathbf{y} \in \Omega, \\ C_h(x_2, y_2) &= \delta_h^2 \exp\left(-\frac{|x_2 - y_2|}{l_h}\right), x_2, y_2 \in [0, 1], \end{aligned}$$

where $\delta_{\text{Ra}}, \delta_h$ denote the respective coefficient of variations and l_{Ra}, l_h denote the respective correlation lengths. The analytic expressions for $\gamma_{\text{Ra},j}, \gamma_{h,j} : j > 0$ are provided in Appendix B. Moreover, in place of the continuity equation, the pressure Poisson equation

$$(4.7) \quad \nabla^T \nabla p(\mathbf{x}, \boldsymbol{\xi}) + \nabla^T \left(\left(\mathbf{u}(\mathbf{x}, \boldsymbol{\xi})^T \nabla \right) \mathbf{u}(\mathbf{x}, \boldsymbol{\xi}) - \text{PrRa}(\mathbf{x}, \boldsymbol{\xi}_1) T(\mathbf{x}, \boldsymbol{\xi}) \mathbf{e}_2 \right) = 0$$

is used to close the coupled PDE system. Table 1 lists the corresponding numerical values of the deterministic parameters used in this study.

Each component PDE system is spatially discretized using a finite volume method, with linear central-differencing schemes [36], on a uniform grid with $m \times m$ cells. Let $\mathbf{u}'_1, \mathbf{u}'_2, \mathbf{p}', \mathbf{t}' \in$

Table 1

Deterministic parameter values in the thermally-driven cavity flow problem.

Pr	Ra	\bar{T}_h	δ_{Ra}	δ_h	l_{Ra}	l_h
0.71	10^3	1	10	0.5	0.5	0.5

\mathbb{R}^{m^2} denote the respective vectors of cell-centroid horizontal velocity, vertical velocity, pressure and temperature, which solve the nonlinear system

$$\begin{aligned}
 (\mathbf{K}_u + \mathbf{A}(\mathbf{u}'_1, \mathbf{u}'_2)) \mathbf{u}'_1 + \mathbf{B}_1 \mathbf{p}' &= \mathbf{0}, \\
 (\mathbf{K}_u + \mathbf{A}(\mathbf{u}'_1, \mathbf{u}'_2)) \mathbf{u}'_2 + \mathbf{B}_2 \mathbf{p}' - \mathbf{R}(\boldsymbol{\xi}_1) \mathbf{t}' &= \mathbf{0}, \\
 \mathbf{K}_p \mathbf{p}' + \mathbf{C}_1(\mathbf{u}'_1, \mathbf{u}'_2) \mathbf{u}'_1 + \mathbf{C}_2(\mathbf{u}'_1, \mathbf{u}'_2) \mathbf{u}'_2 - \mathbf{S}(\boldsymbol{\xi}_1) \mathbf{t}' &= \mathbf{0}, \\
 (\mathbf{K}_T + \mathbf{A}(\mathbf{u}'_1, \mathbf{u}'_2)) \mathbf{t}' - \mathbf{h}(\boldsymbol{\xi}_2) &= \mathbf{0}.
 \end{aligned}
 \tag{4.8}$$

where each term in Eq. 4.8 denotes its respective discretized operator in the coupled PDE system in Eq. 4.1. Subsequently, we formulate a modular multi-physics setup by separating the momentum and energy components of the coupled algebraic PDE system. As per Eq. 1.1, let $\mathbf{u}_1 = [\mathbf{u}'_1; \mathbf{u}'_2; \mathbf{p}'] \in \mathbb{R}^{3m^2}$, $\mathbf{u}_2 = \mathbf{t}' \in \mathbb{R}^{m^2}$ denote the respective solution variables in the modular algebraic system. The component residuals are defined as follows.

$$\begin{aligned}
 \mathbf{f}_1(\mathbf{u}_1, \mathbf{u}_2, \boldsymbol{\xi}_1) &= \begin{bmatrix} \mathbf{K}_u + \mathbf{A}(\mathbf{u}'_1(\mathbf{u}_1), \mathbf{u}'_2(\mathbf{u}_1)) & \mathbf{0} \\ \mathbf{0} & \mathbf{K}_u + \mathbf{A}(\mathbf{u}'_1(\mathbf{u}_1), \mathbf{u}'_2(\mathbf{u}_1)) \\ \mathbf{C}_1(\mathbf{u}'_1(\mathbf{u}_1), \mathbf{u}'_2(\mathbf{u}_1)) & \mathbf{C}_2(\mathbf{u}'_1(\mathbf{u}_1), \mathbf{u}'_2(\mathbf{u}_1)) \\ \mathbf{B}_1 \\ \mathbf{B}_2 \\ \mathbf{K}_p \end{bmatrix} \mathbf{u}_1 - \begin{bmatrix} \mathbf{0} \\ \mathbf{R}(\boldsymbol{\xi}_1) \\ \mathbf{S}(\boldsymbol{\xi}_1) \end{bmatrix} \mathbf{u}_2, \\
 \mathbf{f}_2(\mathbf{u}_1, \mathbf{u}_2, \boldsymbol{\xi}_2) &= (\mathbf{K}_T + \mathbf{A}(\mathbf{u}'_1(\mathbf{u}_1), \mathbf{u}'_2(\mathbf{u}_1))) \mathbf{u}_2 - \mathbf{h}(\boldsymbol{\xi}_2).
 \end{aligned}
 \tag{4.9}$$

The quantities of interest in this study are the statistics of the fluid velocity and temperature, and the probability density functions (pdfs) of the kinetic energy K and internal energy E , defined as follows. $\forall \boldsymbol{\xi} \in \Xi$,

$$K(\boldsymbol{\xi}) = \frac{1}{2} \left(\int_{\Omega} u_1(\mathbf{x}, \boldsymbol{\xi})^2 d\mathbf{x} + \int_{\Omega} u_2(\mathbf{x}, \boldsymbol{\xi})^2 d\mathbf{x} \right), \quad E(\boldsymbol{\xi}) = \int_{\Omega} T(\mathbf{x}, \boldsymbol{\xi}) d\mathbf{x}.
 \tag{4.10}$$

For this numerical example, two instances (or cases) of our proposed framework were implemented and compared against their corresponding monolithic implementations. The block Gauss-Seidel (BGS) approach with Newton updates in each module. In each instance, the stochastic modules and wrappers corresponding to each implementation were developed as MATLABTM scripts, and tested on a 3.1 GHz Intel i5 workstation with 4GB DDR3 memory capacity.

4.2. Case 1: Intrusive + Intrusive. In this instance, both modules use an intrusive propagation method based on solving the SGS system corresponding to the respective Newton

updates to propagate the gPC coefficient matrices. In the monolithic implementation, each module performs a projection in the global s -dimensional stochastic space, while in the modular framework, each module i performs a projection in its local s_i -dimensional stochastic space. Therefore, in each module, the corresponding restriction maps yield the modular gPC coefficient matrix samples, while the prolongation map is defined according to the pseudospectral recovery method (Theorem 2), using local sparse-grid quadrature rules.

For each implementation, the converged gPC coefficient matrices were obtained for $m = 20$, $s_1 = s_2 = 4$, $p = 4$ and a convergence tolerance of 10^{-8} on the Newton updates. Subsequently, using these matrices we computed the probability distribution functions of K and E , along with the mean and standard deviation of the fluid velocity and temperature. The results are shown in Figures 3, 4 and 5 respectively. Due to the high regularity in the solutions and consequent exponential decay in the gPC approximation error, the results are observed to match accurately within the prescribed tolerance of 10^{-4} , which was chosen according to the gPC approximation error of 1.5×10^{-5} observed in the module-based hybrid framework implementation.

Table 2
Average mean-square errors and wall-times observed in Case 1.

s_1, s_2	p	Monolithic		Modular		Speedup factor
		Error	Wall-time (s)	Error	Wall-time (s)	
3	1	8.2×10^{-2}	6	8.8×10^{-2}	8	-0.2
	2	2.2×10^{-3}	27	3.5×10^{-3}	13	1.1
	3	9.3×10^{-5}	181	2.1×10^{-4}	67	1.7
	4	5.4×10^{-6}	1217	1.3×10^{-5}	344	2.5
4	1	9.3×10^{-2}	9	1.2×10^{-1}	10	-0.1
	2	3.3×10^{-3}	53	4.7×10^{-3}	18	1.9
	3	1.3×10^{-4}	742	3.1×10^{-4}	197	2.8
	4	6.1×10^{-6}	7345	1.5×10^{-5}	1625	3.5

Subsequently, for various choices of s_1, s_2, p , we compare the error and computation time in both implementations. In each implementation, the error is as the average mean-square error between the gPC-based surrogate solutions and corresponding deterministic solutions, at 100 random sample points. The results are shown in Table 2. We observe that as for small error tolerances, the costs of module-based intrusive implementation was lower than the monolithic implementation. This can be attributed to the much faster growth in the size of SGS systems with respect to s and p , when the latter approach is implemented.

The highest speedup factor for each instance of s_1, s_2 was observed at the highest order setting ($p = 4$). For $s_1 = s_2 = 3$, we observed a speedup factor of ≈ 2.5 , while for $s_1 = s_2 = 4$, we observed a speedup factor of *approx*3.5. We expect these gains to increase when higher values of p are chosen.

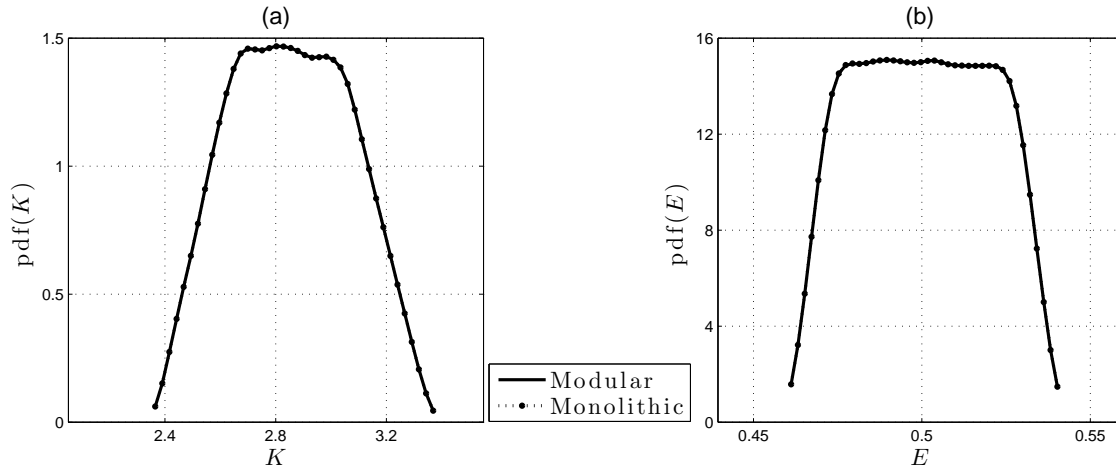


Figure 3. Probability distribution functions of fluid energies computed using both framework implementations. (a) illustrates the kinetic energy K and (b) illustrates the thermal energy E . The KDE method was used to compute the distributions with 10^5 samples of the gPC approximations

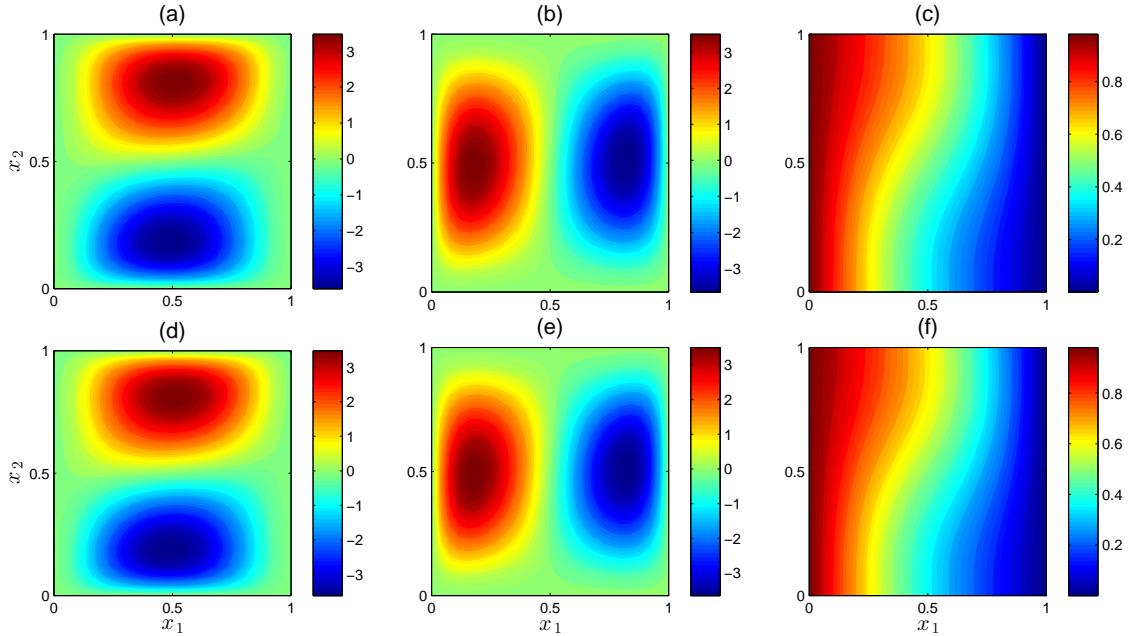


Figure 4. Mean values of solution quantities computed using both framework implementations. Subfigures (a, d), (b, e), (c, f) correspond to u_1 , u_2 , and T respectively, while (a, b, c) and (d, e, f) correspond to the module-based hybrid framework and monolithic framework implementations respectively.

4.3. Case 2: Intrusive + Non-intrusive. In this instance, a non-intrusive variant of module 2, based on the pseudospectral method and corresponding global sparse-grid quadrature rule, is implemented. Due to the nonlinearity in the underlying problem structure, the implementation of this module in the module-based hybrid framework is the same as in the monolithic framework and therefore, no gains in the local computational costs can be expected. However,

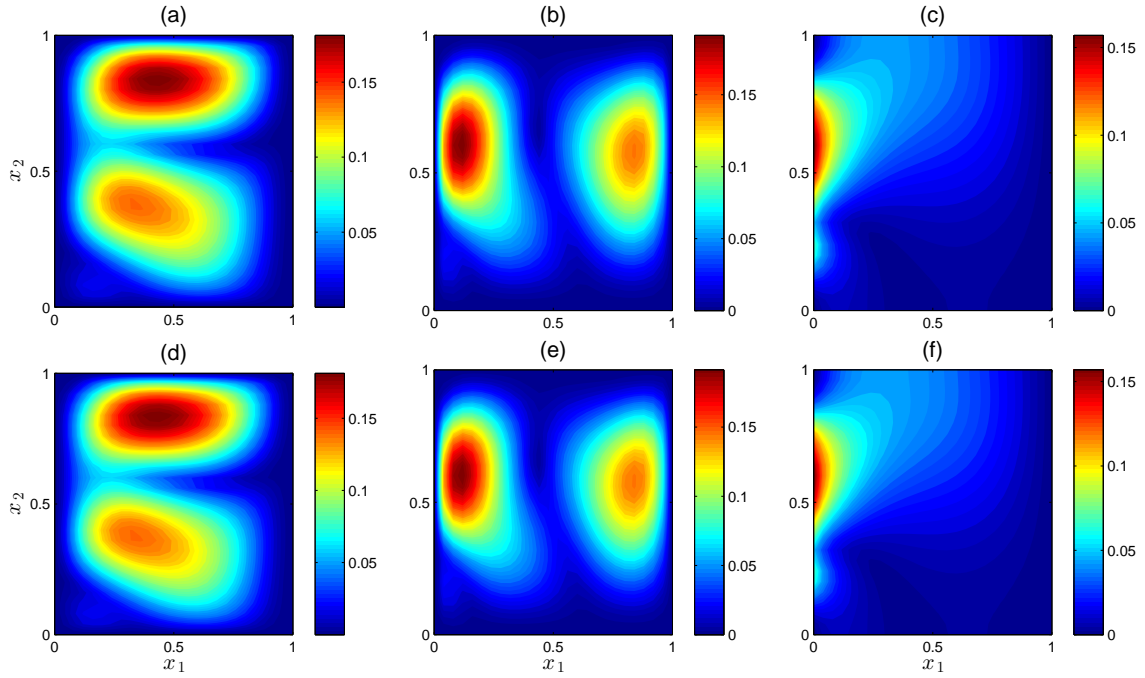


Figure 5. Standard deviation of solution quantities computed using both framework implementations. Sub-figures (a, d), (b, e), (c, f) correspond to u_1 , u_2 , and T respectively, while (a, b, c) and (d, e, f) correspond to the module-based hybrid framework and monolithic framework implementations respectively.

since module 1 is kept unchanged, we would still expect gains in overall computational costs.

Table 3

Mean-square average errors and wall-times observed in Case 2.

s_1, s_2	p	Monolithic		Modular		Speedup factor
		Error	Wall-time (s)	Error	Wall-time (s)	
3	1	1.1×10^{-1}	6	1.3×10^{-1}	7	-0.1
	2	2.6×10^{-3}	23	5.1×10^{-3}	12	0.9
	3	1.0×10^{-4}	166	2.2×10^{-4}	61	1.7
	4	6.5×10^{-6}	1093	1.6×10^{-5}	329	2.3
4	1	1.3×10^{-1}	8	1.5×10^{-1}	9	-0.1
	2	4.1×10^{-3}	46	6.7×10^{-3}	16	1.9
	3	1.8×10^{-4}	671	4.4×10^{-4}	185	2.6
	4	6.8×10^{-6}	6636	2.1×10^{-5}	1521	3.4

For $m = 20$, $s_1 = s_2 = 4$, $p = 4$ and a convergence tolerance of 10^{-8} on the Newton updates, we compared the first two solution moments obtained using both implementations, We observed that the results matched accurately with errors below than the prescribed tolerance

of 10^{-4} , which was chosen according to the gPC approximation error of 2.1×10^{-5} observed in the module-based hybrid framework implementation. When comparing these results to the results obtained in Case 1, we once again observed an accurate match with errors below 10^{-4} .

As in Case 1, s_1, s_2 and p were varied for a comparison of performance. The average mean-square error (computed using 100 samples) and the wall-times observed in both implementations are listed in Table 3. In comparison to Case 1, we observe a slight reduction of costs in both implementations and slight increase in the approximation errors.

Moreover, since module 1 dominates the computational costs, the gains observed in the module-based hybrid implementation were only slightly lower than the gains observed in Case 1. Once, again, for each instance of s_1, s_2 , we observed the highest computational gain at $p = 4$, with higher gains expected as p is further increased. For $s_1 = s_2 = 3$, we observed a speedup factor of ≈ 2.3 , while for $s_1 = s_2 = 4$, we observed a speedup factor of ≈ 3.4 .

5. Conclusions and outlook. We presented an extension of the module-based hybrid UQ framework introduced in our previous work [1] to general nonlinear multi-physics systems. We described the basic components of the framework, namely the restriction and prolongation maps, which facilitates uncertainty propagation to be abstracted down to the module level, and a seamless blending of disparate stochastic modules for efficient global uncertainty propagation. Therefore, our proposed framework reduces the developmental costs and overheads associated with stochastic multi-physics modeling and simulation, when compared to a fully-coupled monolithic framework.

Besides achieving this motivating goal, we observed a speedup factor between 2.3 and 3.5 in numerical experiments, where high order gPC-based propagation methods developed in our proposed framework were compared against their respective monolithic implementations. Due to the nonlinear structure of the model in the numerical example, the gains observed were mainly limited to intrusive modules, where the size of the associated SGS systems were much smaller in the module-based implementation, when compared to the monolithic implementation, for the same global stochastic dimension and gPC order.

Although global multi-variate polynomials were chosen for uncertainty representation in this work, our proposed methodology can also be demonstrated with multiresolution uncertainty propagation schemes which employ either Haar wavelets [37] to overcome the loss of accuracy in models exhibiting discontinuities, or multi-element gPC [38] to overcome the loss of accuracy with long-time integration in unsteady models.

Our experience with this framework has increased our confidence in its viability and superior scalability of modularization over monolithic implementation for uncertainty propagation in complex multi-physics systems. The framework is therefore, a suitable candidate for code-sign in the next generation (exascale) of high performance computers. Efficient strategies for parallelization in the domain of inter-module communication/data transfer, memory manipulation are currently being investigated. Moreover, exploring the interplay between uncertainties and numerical errors at the modular level is also being actively investigated [39].

Acknowledgement. This research was funded by the US Department of Energy, Office of Advanced Computing Research and Applied Mathematics Program and partially funded by the US Department of Energy NNSA ASC Program under Contract No. DE-AC52-07NA27344. The work was performed as a collaboration between Stanford University and the US Depart-

ment of Energy Lawrence Livermore National Laboratory.

REFERENCES

- [1] X. CHEN, B. NG, Y. SUN, AND C. TONG. (2013). *A flexible uncertainty quantification method for linearly coupled multi-physics systems*. J. Comput. Phys., 248, 383-401.
- [2] W. MOROKOFF AND R. CAFLISCH. (1995). *Quasi-monte carlo integration*. J. Comput. Phys., 122(2), 218-230.
- [3] M. MCKAY, R. BECKMAN AND W. J. CONOVER. (1979). *Comparison of three methods for selecting values of input variables in the analysis of output from a computer code*. Technometrics, 21(2), 239-245.
- [4] P. GLYNN AND D. IGLEHART. (1989). *Importance sampling for stochastic simulations*. Manag. Sci., 35(11), 1367-1392.
- [5] R. GHANEM, AND P. SPANOS. (1991). *Stochastic finite elements: a spectral approach* (Vol. 41). New York: Springer.
- [6] D. XIU. (2010). *Numerical methods for stochastic computations: a spectral method approach*. Princeton University Press.
- [7] O. LE MAITRE AND O. KNIO. (2010). *Spectral methods for uncertainty quantification: with applications to computational fluid dynamics*. Springer.
- [8] R. GHANEM. (1998). *Probabilistic characterization of transport in heterogeneous media*. Computer Methods Appl. Mech. and Engrg., 158(3), 199-220.
- [9] O. KNIO AND O. LE MAITRE. (2006). *Uncertainty propagation in CFD using polynomial chaos decomposition*. Fluid Dyn. Res., 38(9), 616-640.
- [10] L. MATHELIN, M. HUSSAINI AND T. ZANG. (2005). *Stochastic approaches to uncertainty quantification in CFD simulations*. Numer. Algorithms, 38(1-3), 209-236.
- [11] B. PHENIX, J. DINARO, M. TATANG, J. TESTER, J. HOWARD AND G. MCRAE. (1998). *Incorporation of parametric uncertainty into complex kinetic mechanisms: application to hydrogen oxidation in supercritical water*. Combustion and Flame, 112(1), 132-146.
- [12] J. LI, AND D. XIU. (2009). *A generalized polynomial chaos based ensemble Kalman filter with high accuracy*. J. Comput. Phys., 228(15), 5454-5469.
- [13] H. ELMAN, C. MILLER, E. PHIPPS, AND R. TUMINARO. (2011). *Assessment of collocation and Galerkin approaches to linear diffusion equations with random data*. Int. J. Uncertain. Quantif., 1(1).
- [14] H. NAJM. (2009). *Uncertainty quantification and polynomial chaos techniques in computational fluid dynamics*. Annu. Rev. Fluid Mech., 41, 35-52.
- [15] S. HOSDER, R. WALTERS AND R. PEREZ. (2006, January). *A non-intrusive polynomial chaos method for uncertainty propagation in CFD simulations*. Proceedings of the 44th AIAA Aerospace Sciences Meeting (Vol. 14, pp. 10649-10667).
- [16] S. HOSDER, R. WALTERS, AND M. BALCH. (2007, April). *Efficient sampling for non-intrusive polynomial chaos applications with multiple uncertain input variables*. Proceedings of the 48th AIAA/ASME/ASCE/AHS/ASC Structures, Structural Dynamics, and Materials Conference, AIAA-2007-1939, Honolulu, HI (Vol. 125).
- [17] D. XIU AND J. HESTHAVEN. (2005). *High-order collocation methods for differential equations with random inputs*. SIAM J. Sci. Comput., 27(3), 1118-1139.
- [18] F. NOBILE, R. TEMPONE AND C. WEBSTER. (2008). *A sparse grid stochastic collocation method for partial differential equations with random input data*. SIAM J. Numer. Anal., 46(5), 2309-2345.
- [19] S. DAS, R. GHANEM AND S. FINETTE. (2009). *Polynomial chaos representation of spatio-temporal random fields from experimental measurements*. J. Comput. Phys., 228(23), 8726-8751.
- [20] G. LOEVEN, J. WITTEVEEN AND H. BIJL. (2007). *A probabilistic radial basis function approach for uncertainty quantification*. Proceedings of AVT-147 Symposium on Computational Uncertainty in Military Vehicles Design.
- [21] T. CHANTRASMI, A. DOOSTAN AND G. IACCARINO. (2009). *Pade-Legendre approximants for uncertainty analysis with discontinuous response surfaces*. J. Comput. Phys., 228(19), 7159-7180.
- [22] A. GIUNTA, J. MCFARLAND L. SWILER AND M. ELDRED. (2006). *The promise and peril of uncertainty*

- quantification using response surface approximations*. Structures and Infrastructure Engineering, 2(3-4), 175-189.
- [23] D. CACUCI, M. IONESCU-BUJOR AND I. NAVON. (2004). *Sensitivity and Uncertainty Analysis: Applications to large-scale systems (Vol. 2)*. CRC Press.
- [24] M. ELDRDRED, L. SWILER AND G. TANG. (2011). *Mixed aleatory-epistemic uncertainty quantification with stochastic expansions and optimization-based interval estimation*. Reliability Engineering & System Safety, 96(9), 1092-1113.
- [25] G. MEDIC, D. YOU AND G. KALTIZIN. (2006). *An approach for coupling RANS and LES in integrated computations of jet engines*. Center for Turbulence Research, Annual Research Briefs, 275-286.
- [26] C. FELIPPA, K. PARK AND C. FARHAT. (2001). *Partitioned analysis of coupled mechanical systems*. Computer Methods Appl. Mech. and Engrg., 190(24), 3247-3270.
- [27] W. GAUTSCHI. (2004). *Orthogonal polynomials: computation and approximation*. Oxford university press.
- [28] D. XIU AND G. KARNIADAKIS. (2002). *The Wiener-Askey polynomial chaos for stochastic differential equations*. SIAM J. Sci. Comput. 24(2), 619-644.
- [29] O. ERNST, A. MUGLER, H. STARKLOFF AND E. ULLMAN. (2012). *On the convergence of generalized polynomial chaos expansions*. ESAIM Math. Model. Numer. Anal, 46(2), 317-339.
- [30] V. EPANECHNIKOV. (1969). *Non-parametric estimation of a multivariate probability density*. Theory of Probability & Its Applications, 14(1), 153-158.
- [31] I. SOBOL. (2001). *Global sensitivity indices for nonlinear mathematical models and their Monte Carlo estimates*. Math. Comput. Simulation, 55(1-3), 271-280.
- [32] A. BJORK. (1996) *Numerical Methods for Least Squares Problems*. ISBN 0-89871-360-9.
- [33] P. CONSTANTINE, M. ELDRDRED, AND E. PHIPPS. (2012). *Sparse pseudospectral approximation method*. Computer Methods Appl. Mech. and Engrg., 229, 1-12.
- [34] O. RUBIO, E. BRAVO, AND J. CLAEYSSEN. (2002). *Thermally driven cavity flow with Neumann condition for the pressure*. Appl. Numer. Math., 40(1), 327-336.
- [35] M. LOEVE. (1955). *Probability Theory. Foundations. Random Sequences*. New York: D. Van Nostrand Company.
- [36] R. LEVEQUE. (2002). *Finite volume methods for hyperbolic problems (Vol. 31)*. Cambridge university press.
- [37] O. LE MAITRE, O. KNIO H. NAJM AND R. GHANEM. (2004). *Uncertainty propagation using Wiener-Haar expansions*. J. Comput. Phys., 197(1), 28-57.
- [38] X. WAN AND G. KARNIADAKIS. (2006). *Multi-element generalized polynomial chaos for arbitrary probability measures*. SIAM J. on Sci. Comput., 28(3), 901-928.
- [39] X. CHEN, J. CONNORS, C. TONG, AND Y. SUN. (2014). *A flexible method to calculate the distributions of discretization errors in operator-split codes with stochastic noise in problem data*. Tech. Report, Lawrence Livermore National Laboratory.

Appendix A.

Lemma A1: . Given a matrix $\mathbf{A} \in \mathbb{R}^{m \times n} : m \geq n$ with $\text{rank}(\mathbf{A}) = n$, $\mathbf{B} = [\mathbf{b}_1 \ \cdots \ \mathbf{b}_k] \in \mathbb{R}^{m \times k}$, and an objective function $f(\mathbf{X}) = \|\mathbf{B} - \mathbf{A}\mathbf{X}\|_F^2 : \mathbb{R}^{n \times k} \rightarrow \mathbb{R}$, the minimizer of f is unique and can be evaluated as follows.

$$(A.1) \quad \mathbf{X}^* = \arg \min_{\mathbf{X} \in \mathbb{R}^{n \times k}} f(\mathbf{X}) = (\mathbf{A}^T \mathbf{A})^{-1} \mathbf{A}^T \mathbf{B}.$$

Proof: . $\forall \mathbf{X} = [\mathbf{x}_1 \ \cdots \ \mathbf{x}_k] \in \mathbb{R}^{n \times k}$, we have

$$(A.2) \quad \begin{aligned} f(\mathbf{x}) &= \|\mathbf{B} - \mathbf{A}\mathbf{X}\|_F^2 \\ &= \left\| \begin{bmatrix} \mathbf{b}_1 \\ \vdots \\ \mathbf{b}_k \end{bmatrix} - (\mathbf{I}_k \otimes \mathbf{A}) \begin{bmatrix} \mathbf{x}_1 \\ \vdots \\ \mathbf{x}_k \end{bmatrix} \right\|_2^2. \end{aligned}$$

The minimizer of f can be obtained by solving $\frac{\partial f}{\partial \mathbf{x}_j} = \mathbf{0} : 1 \leq j \leq k$. Therefore, we have

$$(A.3) \quad \begin{aligned} \begin{bmatrix} \mathbf{x}_1^* \\ \vdots \\ \mathbf{x}_k^* \end{bmatrix} &= \left((\mathbf{I}_k \otimes \mathbf{A})^T (\mathbf{I}_k \otimes \mathbf{A}) \right)^{-1} (\mathbf{I}_k \otimes \mathbf{A})^T \begin{bmatrix} \mathbf{b}_1 \\ \vdots \\ \mathbf{b}_k \end{bmatrix} \\ &= (\mathbf{I}_k \otimes (\mathbf{A}^T \mathbf{A}))^{-1} (\mathbf{I}_k \otimes \mathbf{A}^T) \begin{bmatrix} \mathbf{b}_1 \\ \vdots \\ \mathbf{b}_k \end{bmatrix} \\ &= (\mathbf{I}_k \otimes (\mathbf{A}^T \mathbf{A})^{-1}) (\mathbf{I}_k \otimes \mathbf{A}^T) \begin{bmatrix} \mathbf{b}_1 \\ \vdots \\ \mathbf{b}_k \end{bmatrix} \\ &= (\mathbf{I}_k \otimes ((\mathbf{A}^T \mathbf{A})^{-1} \mathbf{A}^T)) \begin{bmatrix} \mathbf{b}_1 \\ \vdots \\ \mathbf{b}_k \end{bmatrix}, \end{aligned}$$

which can be rewritten as follows.

$$(A.4) \quad \begin{aligned} \mathbf{X}^* = [\mathbf{x}_1^* \ \cdots \ \mathbf{x}_k^*] &= (\mathbf{A}^T \mathbf{A})^{-1} \mathbf{A}^T [\mathbf{b}_1 \ \cdots \ \mathbf{b}_k] \\ &= (\mathbf{A}^T \mathbf{A})^{-1} \mathbf{A}^T \mathbf{B}. \end{aligned}$$

□

Lemma A2: . If the quadrature rule $\left\{ \left(\boldsymbol{\xi}^{(j)}, w^{(j)} \right) \right\}_{j=1}^Q$ can exactly integrate polynomials with total degree $\leq 2p$ then the gPC coefficient matrix $\hat{\mathbf{U}}^p$ obtained using the pseudospectral

formula in Eq. 2.11 corresponds to the unique stationary point of the following objective function.

$$(A.5) \quad f(\hat{\mathbf{Y}}) = \left\| \mathbf{U} - \hat{\mathbf{Y}} \boldsymbol{\Psi} \right\|_{F, \mathbf{W}}^2 : \mathbb{R}^{n \times (P+1)} \rightarrow \mathbb{R},$$

where $\forall \mathbf{X} = [\mathbf{x}_1 \ \cdots \ \mathbf{x}_Q] \in \mathbb{R}^{n \times Q}$, $\|\mathbf{X}\|_{F, \mathbf{W}}^2$ denotes the \mathbf{W} -weighted Frobenius pseudonorm as follows.

$$(A.6) \quad \|\mathbf{X}\|_{F, \mathbf{W}^Q} = \sqrt{\sum_{j=1}^Q w^{(j)} \|\mathbf{x}_j\|_2^2}.$$

Proof.: $\forall \hat{\mathbf{Y}} = [\hat{\mathbf{y}}^0 \ \cdots \ \hat{\mathbf{y}}^P] \in \mathbb{R}^{n \times (P+1)}$, we have

$$(A.7) \quad f(\hat{\mathbf{Y}}) = \left\| \begin{bmatrix} \mathbf{u}^{(1)} \\ \vdots \\ \mathbf{u}^{(Q)} \end{bmatrix} - (\boldsymbol{\Psi}^T \otimes \mathbf{I}_n) \begin{bmatrix} \hat{\mathbf{y}}^0 \\ \vdots \\ \hat{\mathbf{y}}^P \end{bmatrix} \right\|_{\mathbf{W} \otimes \mathbf{I}_n}^2,$$

where

$$(A.8) \quad \forall \begin{bmatrix} \mathbf{x}_1 \\ \vdots \\ \mathbf{x}_Q \end{bmatrix} \in \mathbb{R}^{nQ}, \left\| \begin{bmatrix} \mathbf{x}_1 \\ \vdots \\ \mathbf{x}_Q \end{bmatrix} \right\|_{\mathbf{W} \otimes \mathbf{I}_n} = \left\| [\mathbf{x}_1 \ \cdots \ \mathbf{x}_Q] \right\|_{F, \mathbf{W}}.$$

The unique stationary point of f can be obtained by solving $\frac{\partial f}{\partial \hat{\mathbf{y}}^j} = \mathbf{0} : 1 \leq j \leq Q$. Since the quadrature rule has exact accuracy for polynomials of total degree greater than equal to $2p$, we have

$$(A.9) \quad \sum_{j=1}^Q w^{(j)} \psi^k(\boldsymbol{\xi}^{(j)}) \psi^l(\boldsymbol{\xi}^{(j)}) = \delta_{kl} \Rightarrow \boldsymbol{\Psi} \mathbf{W} \boldsymbol{\Psi}^T = \mathbf{I}_{P+1}.$$

Therefore, we have

$$\begin{aligned}
\begin{bmatrix} \hat{\mathbf{u}}^0 \\ \vdots \\ \hat{\mathbf{u}}^P \end{bmatrix} &= \left((\boldsymbol{\Psi}^T \otimes \mathbf{I}_n)^T (\mathbf{W} \otimes \mathbf{I}_n) (\boldsymbol{\Psi}^T \otimes \mathbf{I}_n) \right)^{-1} \\
&\quad \times (\boldsymbol{\Psi}^T \otimes \mathbf{I}_n)^T (\mathbf{W} \otimes \mathbf{I}_n) \begin{bmatrix} \mathbf{u}^{(1)} \\ \vdots \\ \mathbf{u}^{(Q)} \end{bmatrix} \\
&= (\boldsymbol{\Psi} \mathbf{W} \boldsymbol{\Psi}^T \otimes \mathbf{I}_n)^{-1} (\boldsymbol{\Psi}^T \otimes \mathbf{I}_n)^T (\mathbf{W} \otimes \mathbf{I}_n) \begin{bmatrix} \mathbf{u}^{(1)} \\ \vdots \\ \mathbf{u}^{(Q)} \end{bmatrix} \\
&= (\mathbf{I}_{P+1} \otimes \mathbf{I}_n)^{-1} ((\boldsymbol{\Psi} \mathbf{W}) \otimes \mathbf{I}_n) \begin{bmatrix} \mathbf{u}^{(1)} \\ \vdots \\ \mathbf{u}^{(Q)} \end{bmatrix} \\
\text{(A.10)} \quad &= ((\boldsymbol{\Psi} \mathbf{W}) \otimes \mathbf{I}_n) \begin{bmatrix} \mathbf{u}^{(1)} \\ \vdots \\ \mathbf{u}^{(Q)} \end{bmatrix},
\end{aligned}$$

which can be rewritten as follows.

$$\begin{aligned}
\hat{\mathbf{U}} = [\hat{\mathbf{u}}^0 \quad \dots \quad \hat{\mathbf{u}}^P] &= [\mathbf{u}^{(1)} \quad \dots \quad \mathbf{u}^{(Q)}] (\boldsymbol{\Psi} \mathbf{W})^T \\
\text{(A.11)} \quad &= \mathbf{U} \mathbf{W} \boldsymbol{\Psi}^T.
\end{aligned}$$

As some of the entries in \mathbf{W} may be negative, defining $\|\cdot\|_{F, \mathbf{W}}^2$ and $\|\cdot\|_{\mathbf{W} \otimes \mathbf{I}_n}^2$ as norms would violate the strict positivity and triangular inequality conditions. Therefore, we have instead defined them as pseudonorms. Nonetheless, since some of the entries in \mathbf{W} must be positive, a unique stationary point that minimizes f along some directions would always exist. \square

Lemma A3.: Let $\mathbf{l}_1 : \mathbb{R}^{n_1+n_2} \times \mathbb{R}^{s_1} \rightarrow \mathbb{R}^{n_1}$ and $\mathbf{l}_2 : \mathbb{R}^{n_1+n_2} \times \mathbb{R}^{s_2} \rightarrow \mathbb{R}^{n_2}$ correspond to linear maps such that $\forall (\boldsymbol{\xi}_1, \boldsymbol{\xi}_2) \in \Xi$,

$$\begin{aligned}
\mathbf{u}_1^{\ell+1}(\boldsymbol{\xi}_1, \boldsymbol{\xi}_2) &= \mathbf{m}_1 \left(\mathbf{u}_1^\ell(\boldsymbol{\xi}_1, \boldsymbol{\xi}_2), \mathbf{u}_2^\ell(\boldsymbol{\xi}_1, \boldsymbol{\xi}_2), \boldsymbol{\xi}_1 \right) = \mathbf{l}_1 \left(\mathbf{y}_1^\ell(\boldsymbol{\xi}_1, \boldsymbol{\xi}_2), \boldsymbol{\xi}_1 \right), \\
\text{(A.12)} \quad \mathbf{u}_2^{\ell+1}(\boldsymbol{\xi}_1, \boldsymbol{\xi}_2) &= \mathbf{m}_2 \left(\mathbf{u}_1^{\ell+1}(\boldsymbol{\xi}_1, \boldsymbol{\xi}_2), \mathbf{u}_2^\ell(\boldsymbol{\xi}_1, \boldsymbol{\xi}_2), \boldsymbol{\xi}_2 \right) = \mathbf{l}_2 \left(\mathbf{y}_2^\ell(\boldsymbol{\xi}_1, \boldsymbol{\xi}_2), \boldsymbol{\xi}_2 \right),
\end{aligned}$$

where $\mathbf{y}_1^\ell = [\mathbf{u}_1^\ell; \mathbf{u}_2^\ell]$ and $\mathbf{y}_2^\ell = [\mathbf{u}_1^{\ell+1}; \mathbf{u}_2^\ell]$. The gPC coefficients of $\mathbf{u}_1^{\ell+1}$ and $\mathbf{u}_2^{\ell+1}$ can be obtained by a decomposition of the projection into $\binom{s_2+p}{p}$ and $\binom{s_1+p}{p}$ subproblems respectively.

Proof.: We consider the first equation in Eq. A.12 corresponding to module 1. Each gPC coefficients of $\mathbf{u}_1^{\ell+1}$ can be obtained by projecting it in Ξ against the respective polynomial

basis. Therefore, $\forall 0 \leq |\mathbf{j}_1| + |\mathbf{j}_2| \leq p$, we have

$$\begin{aligned}
\hat{\mathbf{u}}_1^{\ell+1, \mathbf{j}_1 \mathbf{j}_2} &= \int_{\mathbb{R}^{s_2}} \int_{\mathbb{R}^{s_1}} \mathbf{l}_1 \left(\mathbf{y}_1^\ell (\boldsymbol{\xi}_1, \boldsymbol{\xi}_2), \boldsymbol{\xi}_1 \right) \psi_1^{\mathbf{j}_1} (\boldsymbol{\xi}_1) \psi_2^{\mathbf{j}_2} (\boldsymbol{\xi}_2) d\mathcal{P}_1 (\boldsymbol{\xi}_1) d\mathcal{P}_2 (\boldsymbol{\xi}_2) \\
&= \int_{\mathbb{R}^{s_2}} \int_{\mathbb{R}^{s_1}} \left(\mathbf{l}_1 \left(\sum_{|\mathbf{k}_2|=0}^p \sum_{|\mathbf{k}_1|=0}^{p-|\mathbf{k}_2|} \mathbf{y}_1^{\ell, \mathbf{k}_1 \mathbf{k}_2} \psi_1^{\mathbf{k}_1} (\boldsymbol{\xi}_1) \psi_2^{\mathbf{k}_2} (\boldsymbol{\xi}_2), \boldsymbol{\xi}_1 \right) \psi_1^{\mathbf{j}_1} (\boldsymbol{\xi}_1) \right. \\
&\quad \left. \times \psi_2^{\mathbf{j}_2} (\boldsymbol{\xi}_2) d\mathcal{P}_1 (\boldsymbol{\xi}_1) d\mathcal{P}_2 (\boldsymbol{\xi}_2) \right) \\
&= \sum_{|\mathbf{k}_2|=0}^p \sum_{|\mathbf{k}_1|=0}^{p-|\mathbf{k}_2|} \left(\int_{\mathbb{R}^{s_2}} \int_{\mathbb{R}^{s_1}} \mathbf{l}_1 \left(\hat{\mathbf{y}}_1^{\ell, \mathbf{k}_1 \mathbf{k}_2}, \boldsymbol{\xi}_1 \right) \psi_1^{\mathbf{j}_1} (\boldsymbol{\xi}_1) \psi_1^{\mathbf{k}_1} (\boldsymbol{\xi}_1) \psi_2^{\mathbf{j}_2} (\boldsymbol{\xi}_2) \right. \\
&\quad \left. \times \psi_2^{\mathbf{k}_2} (\boldsymbol{\xi}_2) d\mathcal{P}_1 (\boldsymbol{\xi}_1) d\mathcal{P}_2 (\boldsymbol{\xi}_2) \right) \\
\text{(A.13)} \quad &= \int_{\mathbb{R}^{s_1}} \mathbf{l}_1 \left(\sum_{|\mathbf{k}_1|=0}^{p-|\mathbf{j}_2|} \hat{\mathbf{y}}_1^{\ell, \mathbf{k}_1 \mathbf{j}_2} \psi_1^{\mathbf{k}_1} (\boldsymbol{\xi}_1), \boldsymbol{\xi}_1 \right) \psi_1^{\mathbf{j}_1} (\boldsymbol{\xi}_1) d\mathcal{P}_1 (\boldsymbol{\xi}_1).
\end{aligned}$$

Therefore, to evaluate the gPC coefficients $\{\hat{\mathbf{u}}_1^{\ell+1, \mathbf{j}_1 \mathbf{j}_2} : 0 \leq |\mathbf{j}_1| + |\mathbf{j}_2| \leq p\}$, we would only require the gPC coefficients of \mathbf{u}_1^ℓ and \mathbf{u}_2^ℓ with indices belonging to the set that can be written as $\{\mathbf{k}_1 \mathbf{j}_2 \in \mathbb{N}_0^{s_1} \times \mathbb{N}_0^{s_2} : 0 \leq |\mathbf{k}_1| + |\mathbf{j}_2| \leq p\}$. Since these sets are disjoint, we can decompose the projection integrals into independent subproblems corresponding to different values of \mathbf{j}_2 .

The same procedure can be followed to prove the result for the second equation in Eq. A.12. \square

Lemma A4.: Let $\mathbf{A}_1 : \mathbb{R}^{s_1} \rightarrow \mathbb{R}^{n_1 \times n_1}$ and $\mathbf{b}_1 : \mathbb{R}^{n_1+n_2} \times \mathbb{R}^{s_1} \rightarrow \mathbb{R}^{n_1}$ be the random invertible matrix and linear forcing vector derived from module operator \mathbf{m}_1 . Also, let $\mathbf{A}_2 : \mathbb{R}^{s_2} \rightarrow \mathbb{R}^{n_2 \times n_2}$ and $\mathbf{b}_2 : \mathbb{R}^{n_1+n_2} \times \mathbb{R}^{s_2} \rightarrow \mathbb{R}^{n_2}$ be the random invertible matrix and linear forcing vector derived from module operator \mathbf{m}_2 . Therefore, $\forall (\boldsymbol{\xi}_1, \boldsymbol{\xi}_2) \in \Xi$,

$$\begin{aligned}
\mathbf{A}_1 (\boldsymbol{\xi}_1) \mathbf{u}_1^{\ell+1} (\boldsymbol{\xi}_1, \boldsymbol{\xi}_2) &= \mathbf{A}_1 (\boldsymbol{\xi}_1) \mathbf{m}_1 \left(\mathbf{u}_1^\ell (\boldsymbol{\xi}_1, \boldsymbol{\xi}_2), \mathbf{u}_2^\ell (\boldsymbol{\xi}_1, \boldsymbol{\xi}_2), \boldsymbol{\xi}_1 \right) \\
&= \mathbf{b}_1 \left(\mathbf{y}_1^\ell (\boldsymbol{\xi}_1, \boldsymbol{\xi}_2), \boldsymbol{\xi}_1 \right), \\
\mathbf{A}_2 (\boldsymbol{\xi}_2) \mathbf{u}_2^{\ell+1} (\boldsymbol{\xi}_1, \boldsymbol{\xi}_2) &= \mathbf{A}_2 (\boldsymbol{\xi}_2) \mathbf{m}_2 \left(\mathbf{u}_1^{\ell+1} (\boldsymbol{\xi}_1, \boldsymbol{\xi}_2), \mathbf{u}_2^\ell (\boldsymbol{\xi}_1, \boldsymbol{\xi}_2), \boldsymbol{\xi}_2 \right) \\
\text{(A.14)} \quad &= \mathbf{b}_2 \left(\mathbf{y}_2^\ell (\boldsymbol{\xi}_1, \boldsymbol{\xi}_2), \boldsymbol{\xi}_2 \right),
\end{aligned}$$

where $\mathbf{y}_1^\ell = [\mathbf{u}_1^\ell; \mathbf{u}_2^\ell]$ and $\mathbf{y}_2^\ell = [\mathbf{u}_1^{\ell+1}; \mathbf{u}_2^\ell]$. The stochastic Galerkin system (SGS) associated with the gPC coefficients of $\mathbf{u}_1^{\ell+1}$ and $\mathbf{u}_2^{\ell+1}$ can be decomposed into $\binom{s_2+p}{p}$ and $\binom{s_1+p}{p}$ subproblems respectively.

Proof.: We consider the the first equation in Eq. A.14 and its corresponding SGS. The left hand matrix of this system would have $\binom{s_2+p}{p} \times \binom{s_1+p}{p}$ submatrix blocks of size $n_1 \times n_1$ each.

The $(\mathbf{j}_1 \mathbf{j}_2, \mathbf{k}_1 \mathbf{k}_2)$ -th block can be evaluated as follows.

$$(A.15) \quad \begin{aligned} & \int_{\mathbb{R}^{s_2}} \int_{\mathbb{R}^{s_1}} \mathbf{A}_1(\boldsymbol{\xi}_1) \psi_1^{\mathbf{j}_1}(\boldsymbol{\xi}_1) \psi_2^{\mathbf{j}_2}(\boldsymbol{\xi}_2) \psi_1^{\mathbf{k}_1}(\boldsymbol{\xi}_1) \psi_2^{\mathbf{k}_2}(\boldsymbol{\xi}_2) d\mathcal{P}_1(\boldsymbol{\xi}_1) d\mathcal{P}_2(\boldsymbol{\xi}_2) \\ &= \begin{cases} \int_{\mathbb{R}^{s_1}} \mathbf{A}_1(\boldsymbol{\xi}_1) \psi_1^{\mathbf{j}_1}(\boldsymbol{\xi}_1) \psi_1^{\mathbf{k}_1}(\boldsymbol{\xi}_1) d\mathcal{P}_1(\boldsymbol{\xi}_1) & \mathbf{j}_2 = \mathbf{k}_2 \\ \mathbf{0} & \mathbf{j}_2 \neq \mathbf{k}_2 \end{cases}. \end{aligned}$$

The right hand vector would have $\binom{s+p}{p}$ subvector blocks of size n_1 each. The $(\mathbf{j}_1 \mathbf{j}_2)$ -th block can be evaluated using Theorem 1 as follows.

$$(A.16) \quad \begin{aligned} & \int_{\mathbb{R}^{s_2}} \int_{\mathbb{R}^{s_1}} \mathbf{l}_1(\mathbf{y}_1^\ell(\boldsymbol{\xi}_1, \boldsymbol{\xi}_2), \boldsymbol{\xi}_1) \psi_1^{\mathbf{j}_1}(\boldsymbol{\xi}_1) \psi_2^{\mathbf{j}_2}(\boldsymbol{\xi}_2) d\mathcal{P}_1(\boldsymbol{\xi}_1) d\mathcal{P}_2(\boldsymbol{\xi}_2) \\ &= \int_{\mathbb{R}^{s_1}} \mathbf{l}_1\left(\sum_{|\mathbf{k}_1|=0}^{p-|\mathbf{j}_2|} \hat{\mathbf{y}}_1^{\ell, \mathbf{k}_1 \mathbf{j}_2} \psi_1^{\mathbf{k}_1}(\boldsymbol{\xi}_1), \boldsymbol{\xi}_1\right) \psi_1^{\mathbf{j}_1}(\boldsymbol{\xi}_1) d\mathcal{P}_1(\boldsymbol{\xi}_1). \end{aligned}$$

Therefore, the block diagonal structure of the left hand matrix, as indicated by Eq. A.15, and the independence of each subvector in the right hand vector, as indicated by Eq. A.16, is used for decomposing the SGS into smaller subsystems of linear equations. In each subsystem, for various values of $\mathbf{j}_2 \in \mathbb{N}_0^{s_2}$, we can independently compute $\{\hat{\mathbf{u}}_1^{\ell+1, \mathbf{k}_1 \mathbf{j}_2} : 0 \leq |\mathbf{k}_1| \leq p - |\mathbf{j}_2|\}$. The same procedure can be followed to prove the result for the second equation in Eq. A.14. \square

Appendix B.

Karhunen-Loeve expansion for the exponential kernel. Given an n -dimensional spatial domain $\Omega \subseteq \mathbb{R}^n$, let $C_u : \Omega \rightarrow \mathbb{R}^+$ denote the exponential covariance kernel of a spatially varying random quantity $u : \Omega \rightarrow \mathbb{R}$. Therefore, $C_u : \forall \mathbf{x} = [x_1 \ \cdots \ x_n]^\mathbf{T}, \mathbf{y} = [y_1 \ \cdots \ y_n]^\mathbf{T} \in \Omega$,

$$(B.1) \quad C_u(\mathbf{x}, \mathbf{y}) = \exp\left(-\frac{\|\mathbf{x} - \mathbf{y}\|_1}{l}\right) = \prod_{j=1}^n \exp\left(-\frac{|x_j - y_j|}{l}\right),$$

where l denotes the correlation length. Subsequently, we can define the KL expansion of u using an infinite set of random variables $\{\xi_j : j \in \mathbb{N}^n\}$ as follows. $\forall \mathbf{x} \in \Omega$,

$$(B.2) \quad \begin{aligned} u(\mathbf{x}) - \bar{u}(\mathbf{x}) &= \sum_{j \in \mathbb{R}^n} \gamma_j(\mathbf{x}) \xi_j \\ &= \sum_{j_1 \in \mathbb{R}} \cdots \sum_{j_n \in \mathbb{R}} \gamma_{j_1 \dots j_n}(\mathbf{x}) \xi_{j_1 \dots j_n} \\ &= \sum_{j_1 \in \mathbb{R}} \cdots \sum_{j_n \in \mathbb{R}} \prod_{k=1}^n g_{j_k}(r_k) \xi_{j_1 \dots j_n} \end{aligned}$$

where $\forall j > 0$, if ζ_j solves

$$(B.3) \quad l\zeta_j + \tan\left(\frac{\zeta_j}{2}\right) = 0,$$

and $\zeta_{j+1} > \zeta_j > 0$, then $\forall x \in \mathbb{R}$,

$$(B.4) \quad g_j(x) = \begin{cases} 2\sqrt{\frac{l\zeta_j}{1+l^2\zeta_j^2}} \frac{\cos(\zeta_j x)}{\sqrt{\zeta_j + \sin(\zeta_j)}} & j \text{ is odd,} \\ 2\sqrt{\frac{l\zeta_j}{1+l^2\zeta_j^2}} \frac{\sin(\zeta_j x)}{\sqrt{\zeta_j - \sin(\zeta_j)}} & j \text{ is even.} \end{cases}$$

Therefore, as is required in §4, a truncated KL expansion can be easily obtained from the single index form of the expansion in Eq. B.2.